Eur. Phys. J. C (2024) 84:293
https://doi.org/10.1140/epjc/s10052-024-12652-6

THE EUROPEAN PHYSICAL JOURNAL C

Regular Article - Theoretical Physics

Electromagnetic field on the complexity of minimally deformed compact stars

Abeer M. Albalahi[1,a], **M. Z. Bhatti**[2,b], **Akbar Ali**[1,c], **S. Khan**[2,d]

[1] Department of Mathematics, College of Science, University of Ha'il, Ha'il, Kingdom of Saudi Arabia
[2] Department of Mathematics, University of the Punjab, Quaid-i-Azam Campus, Lahore 54590, Pakistan

Received: 14 February 2024 / Accepted: 3 March 2024 / Published online: 20 March 2024

Abstract In the context of this endeavor, we establish a simple protocol for formulating interior stellar solutions that exhibit spherically symmetric configurations against the backdrop of relativistic gravitational decoupling through radial metric deformation (minimal geometric deformation scheme). In this pursuit, we make use of the vanishing complexity factor ($\widetilde{Y}_{TF}$) condition, based on Herrera's (Phys Rev D 97, 044010, 2018) innovative concept regarding the complexity of static or slowly evolving spherical matter configurations. The idea of a complexity factor emerges as the outcome of the orthogonal splitting of the Riemann–Christoffel tensor, which yields different scalar functions, known as structure scalars. The protocol is demonstrated by employing the Buchdahl and Tolman relativistic stellar ansatzes as isotropic seeds. Both of these ansatzes exhibit similar physical features, with a minor variation in their magnitudes in the case of $\widetilde{Y}_{TF} \neq 0$, where $0 \leq \alpha < 1$, and α represents a coupling parameter. However, when $\widetilde{Y}_{TF} = 0$, the Buchdahl stellar ansatz exhibits a uniform density matter configuration, while the Tolman model features an increasing pressure profile. The obtained relativistic stellar models satisfy the basic viability constraints required for the physically realistic configurations.

1 Introduction

The Einstein field equations (EFEs), $G_{\mu\eta} = \kappa T_{\mu\eta}$, form the foundation of the gravitational theory of relativity (GR), which defines the connection between the spacetime geometry and the distribution of energy within space. The spacetime geometry describing the gravitational interactions in the universe, is represented by the Einstein tensor $G_{\mu\eta}$, while the overall energy content of space is defined by the stress-energy tensor $T_{\mu\eta}$. Undoubtedly, among all relativistic theories, GR provides the most widely accepted understanding of how the gravitational field influences its surroundings. In astrophysics, the understanding of relativistic compact stars holds great significance as they serve as top-notch laboratories for exploring extremely dense matter under extreme conditions. Therefore, modeling the interior configurations of compact objects remains a subject that captivates the keen interest of researchers. In the quest for a model of a self-gravitational compact configuration, the first step involves identifying exact and closed-form solutions to EFEs. However, acquiring exact solutions becomes challenging due to the inherent non-linearity in the EFEs. Researchers have conducted numerous investigations to establish conditions that not only allow the closure of the relativistic system but also simultaneously yield real physical models capable of describing compact configurations. In this respect, various conditions are introduced through state equations to represent the fundamental structural features of relativistic fluids constituting compact stars. However, alternative possibilities, such as employing reasonable heuristic conditions on metric potentials, also exist and effectively contribute to closing and solving the gravitational equations of motion. Furthermore, constraints can be applied to the spacetime manifold, such as the Karmarkar condition, which limits the Riemann-Christoffel tensor $R_{\mu\eta\gamma\delta}$ to account for the embedding into a 5-dimensional flat spacetime. By adopting this approach, we can consider the relevant complexity-notion within the domain of GR for relativistic stellar fluids. This condition provides additional information that can be employed to classify the relativistic system. In this pursuit, several gravitational solutions based on isotropic fluid distributions have

[a] e-mail: a.albalahi@uoh.edu.sa
[b] e-mail: mzaeem.math@pu.edu.pk (corresponding author)
[c] e-mail: ak.ali@uoh.edu.sa
[d] e-mail: suraj.pu.edu.pk@gmail.com

been formulated with different gravitational models in various contexts [2–4].

The assumption of "local isotropy" is generally employed in the study of spherical compact fluid configurations for approximating the interior gravitational field of these systems. The term local isotropy refers to a physical phenomenon where the measurement of pressure is independent of direction, giving rise to spherical perfect fluid configurations. This Pascal-like characteristic of the fluid distribution is supported by extensive experimental findings. The perfect fluid distributions, whether Newtonian or relativistic, are considered as the initial approximations in constructing physically viable compact systems. Due to the significance of these models, general solutions characterizing perfect fluid configurations with spherical symmetry in Einstein's GR have been formulated over the past several years. Schwarzschild [5] developed the pioneering solution for a slowly evolving stellar configuration with uniform density, employing a perfect fluid as a gravitational source in 1918. He formulated two analytical solutions to EFEs: the "exterior solution", which is pertinent outside the stellar distribution, and the "interior solution", serving as an approximation for what occurs within the star.

However, compelling theoretical evidence leads astrophysicists to believe that stellar configurations with nuclear density, ($> 10^{15}\text{g/cm}^3$), exhibit local anisotropy. This leads to the formation of anisotropic fluid spheres in which $P_r \neq P_\perp$, where P_r and $P_\perp$ denote radial and tangential stresses, respectively. The classical work by Jeans [6] introduced the concept of anisotropic stresses in low-density relativistic gravitational sources, such as spherical galactic structures, arising from anisotropic velocity distributions. Bowers and Liang [7] conducted a ground-breaking investigation into the effects of unequal principal stresses on the structural characteristics of self-gravitational compact spheres. Ruderman [8] pointed out that in the relativistic regime, matter will deviate from its isotropic nature, and anisotropic features will enrich its composition. The presence of anisotropy is believed to contribute to the formation of more compact configurations. Furthermore, Herrera and Santos [9] carried out a comprehensive investigation to explore the relevance of pressure anisotropy on relativistic self-gravitational compact systems in the context of GR. Bonnor [10] investigated the dynamics of stellar configurations assuming an electrically charged anisotropic fluid distribution. Additionally, Hillebrandt and Steinmetz [11] examined the stability of anisotropic stresses in stellar structures within the principles of GR. Furthermore, it has been noted in [12] that the emergence of certain types of physical phenomena during the evolution of self-gravitational compact objects will inevitably result in the appearance of anisotropic stresses, even when the configuration is initially isotropic. Since any equilibrium distribution represents the final phase of a dynamic regime, there is no reason to assume the disappearance of pressure anisotropy at the concluding equilibrium phase. Therefore, the final distribution, even if it is originally filled with perfect fluid becomes imperfect. Furthermore, numerous studies have been conducted to acquire interior solutions for electrically charged EFEs linked to both static and non-static anisotropic fluid spheres [13–22].

In stellar configurations, deviations from gravitational isotropy can arise in both extremely high-density and extremely low-density conditions due to various factors. The relativistic gravitational collapse of compact configurations with high density can result from exotic phase transitions [23,24], with one noteworthy example being the pion condensed state [25–28]. By releasing a significant amount of energy and relaxing the state equation, the pion condensed state significantly influences the relativistic collapsing fluids. The authors of [29] emphasized that the configuration of a pion condensed phase could be described by considering anisotropic pressure distributions, which arise from the configuration of the π^- modes. The relevance of anisotropic part of $T_{\mu\eta}$ linked to magnetic field lines within a type-II superconductor, particularly in the context of a neutron stars has been examined in [30,31]. The presence of anisotropic stresses is also linked to the existence of type-P superfluids [8], solid core as well as boson stars [32,33] that are considered as the essential components of realistic stellar configurations. The existence of anisotropic stresses could be attributed to another source, namely, viscosity.

In addition to considering gravitational anisotropy as a key element in understanding the dynamics of both static and non-static compact structures, we can also represent it through a scalar function. This scalar can be defined in terms of a unique connection between $\Delta = P_r - P_\perp$ (anisotropic factor) and the gradient of energy density (density inhomogeneity) and is dubbed as complexity factor. The notion of complexity in physics lacks intuitiveness, making the definition of complexity for various systems a non-trivial task. This concept is connected to numerous fascinating aspects that delve into the structure existing within the system. The term complexity was initially associated with elements such as information and entropy, grounded in the notion of quantifying the fundamental internal structure of a system. For this reason, it has been comprehensively explored by numerous researchers and applied in diverse scientific scenarios [34–39]. Despite extensive study, there remains a lack of consensus on how to precisely define complexity across the diverse features of nature. Generally, the exploration of complexity stems from examining the perfect crystal (characterized by regular behavior) and the isolated ideal gas (exhibiting irregular behavior). These systems serve as examples of the simplest models and, consequently, are considered to have minimal complexity. Since both of these simplest models exhibit extreme behavior within the spectrum of order and informa-

tion, it becomes apparent that the conception of complexity must include some additional factors beyond just order or information.

To address an intuitively "complex" configuration, we should possess the capability to define an observable that can measure and quantify its complexity. This allows us to effectively distinguish between various structures based on their respective degrees of complexity. Therefore, establishing a hierarchy to classify relativistic structures, ranging from the simplest Minkowski metric to more complex radiating stellar fluids, based on their complexity factors is an important task [40]. A crucial groundwork for understanding and comparing the dynamics of different systems could emerge by defining corresponding physical attributes within the framework of such a hierarchy. An intuitive description of complexity related to stellar systems, based on fluid features such as non-uniform energy density and anisotropic stresses, has been proposed by Herrera [1]. In contrast to the definitions of complexity associated with order and information, this new definition is directly linked to the internal configuration of relativistic fluids. More precisely, this alternative description is associated with a scalar quantity (Y_{TF}) resulting from the orthogonal splitting of $R_{\mu\eta\delta\gamma}$ [41,42]. The scalar Y_{TF} is explicitly connected to the internal framework of the fluid distribution and demonstrates the complexity inherent in a self-gravitational compact system. Respective applications of the $Y_{TF} = 0$ constraint in the context of alternative gravitational models are discussed in [43–48].

In seeking closed-form analytical solutions for EFEs, one of the most widely accepted gravitational decoupling techniques in the realm of classical GR is the minimal geometric deformation scheme (MGD-decoupling, thereafter). The basic formalism of MGD-decoupling is based on considering a generic form of fluid distribution, whose stress-energy tensor can be encoded as

$$\widetilde{T}_{\mu\eta} = T_{\mu\eta} + \alpha\Theta_{\mu\eta},$$

where the coupling parameter α is inserted to explore the impacts of Θ-gravitational sector corresponding to the seed source $T_{\mu\eta}$. It is interesting to observe that the addition of these new sources may give rise to other fields including tensor, vector and scalar fields. The MGD-decoupling enables us to solve the EFEs for each gravitational source $\{T_{\mu\eta}, \Theta_{\mu\eta}\}$ independently. The complete solution of the considered system is then obtained through the principle of superposition. This is particularly beneficial when dealing with scenarios that are more complex than trivial ones, i.e., modeling the internal configurations of self-gravitational objects subject to anisotropic matter. Ovella made groundbreaking contributions in formulating consistent solutions to the EFEs using MGD-decoupling against the backdrop of the Randall-Sundrum brane-world [49,50]. Afterwards this systematic scheme was extended generalizing the isotropic fluid configuration into the anisotropic regime. The deformation of the radial metric potential in MGD-decoupling allows us to explore the thermodynamical features associated with compact distributions subject to the Θ-gravitational source [49–51]. The respective applications of MGD-decoupling can be found in the formulation of diverse cosmological and astrophysical solutions. Under the framework of MGD-decoupling, perfect fluid solutions were generalized into an anisotropic regime through the mechanisms of braneworld [52] and GR [53]. check grammar By deforming the established relativistic metric variables, Durgapal–Fuloria [54], Heintzmann [55], Tolman VII [56], Schwarzschild [57] and Krori–Barua [58], physically acceptable stellar models characterizing the anisotropic self-gravitational compact configurations have been constructed. Some more recent investigations on the role of MGD-decoupling in exploring the spherically symmetric stellar configurations can be seen in [59–64].

Herrera et al. [42] developed a systematic approach for exploring the internal features of the astrophysical compact configurations within the principles of GR. They stellar solutions characterizing the evolution and configuration of non-static self-gravitational stellar objects. These equations were expressed through five scalars, namely $\{Y_{TF}, X_{TF}, X_T, Y_T, Z\}$, where Z becomes zero for non-diffusive fluids fluids. It was pointed out that these scalars are closely connected to interior structural features of the matter distribution, such as anisotropic pressure, Tolman mass, and homogeneous as well as non-homogeneous energy density. Specifically, these scalars exhibit the following features:

- The combined aftermath of anisotropic pressure and non-uniform density is encoded in the scalar Y_{TF} [42,65].
- The non-uniformity of the energy density is controlled by X_{TF} [42,65].
- In the equilibrium state, it is found that $Y_T \propto m_T$, where m_T denotes the Tolman mass [42,65].
- X_T characterizes the energy density associated with the relativistic fluids [42,65].

The inclusion of an electric charge influences the evolution of self-gravitational configurations through its explicit presence in the scalar functions, as discussed in [65]. Inspired by the profound physical significance of the aforementioned scalar quantities, we will calculate them using the charged fluid distribution with two different metric ansatzes, namely:

- Buchdahl ansatz.
- Tolman ansatz.

We construct physically acceptable stellar solutions exhibiting the self-gravitational compact spheres by imposing the null-complexity constraint under MGD-decoupling. More precisely, this study delves into investigating the impact

of complexity on slowly evolving or static charged self-gravitational fluids characterized by spherical symmetry. This exploration is carried out through the application of gravitational decoupling within the framework of MGD formalism. This well-established gravitational technique has previously been employed to derive viable configurations for compact stars filled with anisotropic fluid, adhering to well-known metrics. This work is concerned with the theoretical modeling of two well-known metric potentials (Buchdahl and Tolman) by employing the MGD-decoupling by considering electrically charged matter configuration. The MGD-decoupling is considered very beneficial in formulating the solutions associated with stellar configuration by deforming the radial metric potential g_{rr}. This involves the decomposition of the considered system into two sets, one for the $T_{\mu\eta}$-source and the second for the $\Theta_{\mu\eta}$-source. The subsequent sections of this paper are organized as follows: The Einstein–Maxwell relativistic equations under the term of MGD-decoupling are defined in Sect. 2. The basic framework of MGD-decoupling, along with the corresponding expressions of mass functions and the junction condition, is introduced in Sect. 3. In Sect. 4, we employ the Karmarkar condition to construct the structure scalars along with their respective complexity factors within the MGD-decoupling framework. The basic framework of complexity-free condition and the protocol to obtain the anisotropic fluid solutions is presented in Sect. 4. Furthermore, we obtain the decoupled stellar solutions endowed with spherical symmetry for the Buchdahl and Tolman ansatzes obeying the null-complexity constraint in the Sects. 4.1 and 4.2, respectively. A comprehensive physical investigation for the considered metric potentials is presented in Sect. 5. The concluding remarks for both sets of solutions are discussed in Sect. 6.

2 The generic formalism of decoupling

The generic action in the context of electrically charged decoupled stellar structures can be defined as

$$\mathcal{A}_{\mathrm{G}} \equiv \mathcal{A}_{\mathrm{EH}} + \alpha\mathcal{A}_{\mathrm{X}} = \int d^4x\sqrt{|g|}\left(\frac{\mathrm{R}}{16\pi} + \mathscr{L}_e + \mathscr{L}_m + \alpha\mathscr{L}_\Theta\right), \tag{1}$$

where:

- The densities of matter and electric fields are encoded as $\mathscr{L}_m$ and $\mathscr{L}_e$, respectively, while $\mathscr{L}_\Theta$ denotes the fields of new gravitational sector (Θ-gravitational sector, henceforward) not addressed by standard GR.
- $\mathcal{A}_{\mathrm{EH}}$ and $\mathcal{A}_{\mathrm{X}}$ denote the actions associated with Einstein–Maxwell sector and the X-gravitational sector, respectively.
- R denotes the usual curvature scalar, derived by contracting the Ricci curvature tensor $R_{\mu\eta}$.
- The parameter α is the decoupling constant, and $g = tr(g_{\alpha\beta})$, where $g_{\mu\eta}$ is the metric tensor.

The gravitational equations of motion characterizing the decoupled Einstein–Maxwell framework can be defined by varying the action (1) with respect to $g_{\mu\eta}$ as

$$G_{\mu\eta} \equiv R_{\mu\eta} - \frac{1}{2}\mathrm{R}g_{\mu\eta} = 8\pi\left(\widetilde{T}_{\mu\eta} + S_{\mu\eta}\right), \tag{2}$$

where $G_{\mu\eta}$ and $S_{\mu\eta}$ symbolize Einstein and electromagnetic tensors, respectively. The stress-energy tensor $\widetilde{T}_{\mu\eta}$ denotes a sum of two different and independent gravitational field sources,

$$\widetilde{T}_{\mu\eta} = T_{\mu\eta} + \alpha\Theta_{\mu\eta}, \tag{3}$$

with

$$(\widetilde{T}_{\mu\eta}) = \mathrm{diag}(\widetilde{\varepsilon}, -\widetilde{P}_r, -\widetilde{P}_\perp, -\widetilde{P}_\perp), \tag{4}$$

where $\widetilde{\varepsilon}$, $\widetilde{P}_r$ and $\widetilde{P}_\perp$ denote effective energy density, effective radial pressure and effective tangential pressure, respectively. The interior of the slowly evolving, charged self-gravitational structure is approximated with perfect fluid distribution. In this respect, the contributions of the seed sector and Θ-gravitational sector can be encoded as

$$\left(T_\eta{}^\mu\right) = \mathrm{diag}\left(\varepsilon, -P, -P, -P\right), \tag{5}$$

$$\left(\Theta_\eta^{\ \mu}\right) = \mathrm{diag}\left(\Theta_0{}^0, -\Theta_1{}^1, -\Theta_2{}^2, -\Theta_3{}^3\right), \tag{6}$$

where $\Theta_\eta^{\ \mu}$ denotes a specific type of unknown standard fluid distribution induced by the decoupling parameter α. Now, the effective variables appearing in Eqs. (4)–(6) are identified as

$$\widetilde{\varepsilon} = T_0{}^0 + \alpha\Theta_0{}^0 \equiv \varepsilon + \varepsilon^\Theta, \tag{7}$$

$$\widetilde{P}_r = -T_1{}^1 - \alpha\Theta_1{}^1 \equiv P + P_r^\Theta, \tag{8}$$

$$\widetilde{P}_\perp = -T_2{}^2 - \alpha\Theta_2{}^2 \equiv P + P_\perp^\Theta. \tag{9}$$

Now, it becomes evident that the inclusion of the Θ-gravitational source induces anisotropy within the charged self-gravitational compact system, as defined by its structural parameters

$$\Delta^{eff} \equiv \widetilde{P}_r - \widetilde{P}_\perp = -\alpha(\Theta_2{}^2 - \Theta_1{}^1), \quad \Theta_1{}^1 \neq \Theta_2{}^2. \tag{10}$$

Next, consider the following ansatz

$$ds^2 = g_{\mu\eta}dx^{\mu}dx^{\eta}, \quad (g_{\mu\eta}) = \text{diag}\left(e^{\nu(r)}, -e^{\lambda(r)}, -r^2, -r^2\sin^2\theta\right), \tag{11}$$

for time-independent spherically symmetric manifold, with Schwarzschild-like coordinates $x^{0,1,2,3} = t, r, \theta, \varphi$, respectively. The stress-energy tensor describing the electromagnetic interactions within the compact configuration can be defined as

$$S_{\mu\eta} = \frac{1}{4\pi}\left(F_{\mu}^{\ \gamma}F_{\eta\gamma} + \frac{1}{4}g_{\mu\eta}F_{\gamma\delta}F^{\gamma\delta}\right), \quad \text{with} \quad F_{\mu\eta} = \partial_{\mu}\phi_{\eta} - \partial_{\eta}\phi_{\mu}, \tag{12}$$

where ϕ_{μ} is the four potential, which in the static case reads $\phi_{\mu} = (\Psi, 0, 0, 0)$ with $\Psi \equiv \Psi(r)$. As the electromagnetic tensor $F_{\mu\eta}$ obeys the Maxwell's electromagnetic field equations

$$\nabla_{\eta}\left[(-g)^{1/2}F^{\mu\eta}\right] = 4\pi(-g)^{1/2}J^{\mu}, \tag{13}$$

$$\partial_{[\gamma}F_{\mu\eta]} = 0, \tag{14}$$

where the four-current J^{μ} reads

$$J^{\mu} = \Phi V^{\mu}, \tag{15}$$

where $\Phi \equiv \Phi(r)$ being the density of electric charge. Subsequently, for the system (11), the Maxwell's equations can be reformulated into the following form

$$\Psi'' + \frac{1}{2r}\left[4 - r(\nu' + \lambda')\right]\Psi' = 4\pi\Phi e^{(\lambda+\nu/2)}, \tag{16}$$

whose integration with respect to r reads

$$\Psi' = \frac{s}{r^2}e^{(\nu+\lambda)/2}, \quad \text{with} \quad s(r) = 4\pi\int_0^r \Phi e^{\mu/2}u^2du, \tag{17}$$

where an overhead prime denotes r-derivative, while $s(r)$ is the total electric charge present inside the spherically symmetric compact configuration. Finally, the non-zero components of $S_{\mu\eta}$ read

$$S_0^{\ 0} = S_1^{\ 1} = -S_2^{\ 2} = -S_3^{\ 3} = \frac{s^2}{8\pi r^4}. \tag{18}$$

Thus, the non-null constituents associated with electrically charged EFEs are defined as

$$\widetilde{\varepsilon} + S_0^{\ 0} = \frac{1}{8\pi}\left[\frac{1}{r^2} - \left(\frac{1}{r^2} - \frac{\lambda'}{r}\right)e^{-\lambda}\right], \tag{19}$$

$$\widetilde{P}_r + S_1^{\ 1} = \frac{1}{8\pi}\left[-\frac{1}{r^2} + \left(\frac{1}{r^2} + \frac{\lambda'}{r}\right)e^{-\lambda}\right], \tag{20}$$

$$\widetilde{P}_{\perp} + S_2^{\ 2} = \frac{1}{8\pi}\left[\frac{\lambda''}{2}e^{-\lambda} - (\lambda' - \nu')\left(\frac{\nu'}{4} + \frac{1}{2r}\right)e^{-\lambda}\right]. \tag{21}$$

The stress-energy tensor obeys the conservation condition

$$\left(\widetilde{T}_{\eta}^{\ \mu} + S_{\eta}^{\ \mu}\right)_{;\mu} \equiv 0. \tag{22}$$

If we take $\mu = 1$ in the above equation, then after some manipulations, we get

$$\begin{aligned} 0 = &\left(\widetilde{T}_1^{\ 1} + S_1^{\ 1}\right)' - \frac{1}{2}g^{00}\left(g_{00}\right)' \times \left(\widetilde{T}_0^{\ 0} + S_0^{\ 0} - \widetilde{T}_0^{\ 0} - S_0^{\ 0}\right) - g^{22}\left(g_{11}\right)' \left(\widetilde{T}_2^{\ 2} + S_2^{\ 2} - \widetilde{T}_2^{\ 2} - S_2^{\ 2}\right) \\ 0 = &\left(T_1^{\ 1} + S_1^{\ 1}\right)' - \frac{\nu'}{2}\left(T_0^{\ 0} + S_0^{\ 0} - T_1^{\ 1} - S_1^{\ 1}\right) - \frac{2}{r}\left(T_2^{\ 2} + S_2^{\ 2} - T_1^{\ 1} - S_1^{\ 1}\right) + \alpha\mathcal{F}\left(\Theta_{\mu}^{\ \mu}\right), \end{aligned} \tag{23}$$

where

$$\mathcal{F}\left(\Theta_{\mu}^{\ \mu}\right) \equiv \left[\left(\Theta_1^{\ 1}\right)' - \frac{\nu'}{2}\left(\Theta_0^{\ 0} - \Theta_1^{\ 1}\right) - \frac{2}{r}\left(\Theta_2^{\ 2} - \Theta_1^{\ 1}\right)\right]. \tag{24}$$

The above gravitational system reduces to the isotropic charged stellar distribution by assuming $\alpha = 0$. In the next section, we employ the Ovalle's MGD-approach [66], which splits the original system into two arrays.

3 The notion of minimal geometric deformation

The gravitational decoupling is a widely recognized mathematical framework that enables us to disintegrate the complex gravitational source and to develop a well-behaved anisotropic gravitational solutions form the perfect fluid seed sources. It becomes evident that the non-linear nature of the Einstein–Maxwell gravitational sector prevents the decomposition (3), resulting in two separate sets of relativistic systems, each corresponding to the gravitational sources involved. In this respect, we employ the MGD approach to split the considered relativistic system for understanding the effects emerging from the Θ-gravitational source on the electrically charged perfect fluid configuration. Let us consider a transformation of the metric potentials $\left\{e^{\lambda(r)}, e^{\nu(r)}\right\}$ proposed by Ovalle [66], whereby

$$\nu(r) = \omega(r) + \alpha\mathcal{H}(r), \tag{25}$$

$$e^{-\lambda(r)} = \sigma(r) + \alpha\mathcal{G}(r), \tag{26}$$

where α is a real constant controlling the effects of $\Theta_{\mu\eta}$ on the source $T_{\mu\eta}$, while $\{\mathcal{G}, \mathcal{H}\}$ are the deformation functions. The MGD-approach assumes deformation only in the radial metric potential $e^{\lambda(r)}$, implying $\mathcal{H}(r) = 0$ and $\mathcal{G}(r) \neq 0$. Therefore, employing the above-mentioned deformations, we obtain two sets of relativistic gravitational systems

$$\varepsilon + \frac{s^2}{8\pi r^4} = \frac{1}{8\pi}\left(\frac{1-\sigma'}{r^2} - \frac{\sigma'}{r}\right), \tag{27}$$

$$P - \frac{s^2}{8\pi r^4} = \frac{1}{8\pi}\left(\frac{1-\sigma'}{r^2} - \frac{\sigma'\omega'}{r}\right), \tag{28}$$

$$P + \frac{s^2}{8\pi r^4} = \frac{1}{8\pi}\left[\left(\frac{\sigma'\omega'}{4} + \frac{\sigma'}{2r}\right) + \frac{\sigma}{2}\left(\omega'' + \frac{\omega'}{r} + \frac{\omega'^2}{2}\right)\right]. \tag{29}$$

Then, using the isotropic condition, we can calculate the electric field for the charged system as

$$\frac{s^2}{r^4}7 = \frac{1}{8r^2}\Big(2r^2\sigma\omega'' + r^2\sigma\omega'^2 + 2r\sigma\omega' + r^2\sigma'\omega' + 2r\sigma' - 4r\sigma' - 4\sigma + 4\Big). \tag{30}$$

The solution for the electrically charged seed gravitational source with $\alpha = 0$ can be described by the following metric

$$ds^2 = g_{\mu\eta}dx^\mu dx^\eta, \quad (g_{\mu\eta}) = \text{diag}\left(e^{\omega(r)}, 1/\sigma(r), -r^2, -r^2\sin^2\theta\right). \tag{31}$$

The gravitational equations associated with the additional gravitational sector $\Theta_{\mu\eta}$ can be defined as

$$8\pi\varepsilon^\Theta = -\alpha\left(\frac{\mathcal{G}'}{r} + \frac{\mathcal{G}}{r^2}\right), \tag{32}$$

$$8\pi P_r^\Theta = \alpha\mathcal{G}\left(\frac{1}{r^2} + \frac{\omega'}{r}\right), \tag{33}$$

$$8\pi P_\perp^\Theta = \frac{\alpha\mathcal{G}}{2}\left(\omega'' + \frac{\omega'^2}{2} + \frac{\omega'}{r}\right) - \frac{\alpha\mathcal{G}'}{2}\left(\frac{\omega'}{2} + \frac{1}{r}\right). \tag{34}$$

The relativistic hydrostatic equilibrium equations associated with $\left[T_\eta^{\ \mu} + S_\eta^{\ \mu}\right]$ and $\Theta_\eta^{\ \mu}$ fluid sources take the following forms

$$P' + \frac{4\pi r^4 P - r m_0 + s^2}{r(r^2 - 2rm_0 + s^2)}(\varepsilon + P) = \frac{ss'}{4\pi r^4}, \tag{35}$$

and

$$\left(P_r^\Theta\right)' + \frac{m_0 + 4\pi r^3\widetilde{P}_r}{(r - m_0 s)}\left(\varepsilon^\Theta + P_r^\Theta\right) = -\frac{2\Delta^{eff}}{r}, \tag{36}$$

where the relativistic mass function m_0 reads [67–69]

$$m_0 \equiv \left(\frac{r}{2}\right)R^3_{232} + \frac{s^2}{2r} = \frac{r}{2}(1-\sigma) + \frac{s^2}{2r}. \tag{37}$$

Then, we have

$$m = m_0(r) - \frac{r\alpha}{2}h(r). \tag{38}$$

The expression of the relativistic geometric mass associated with decoupled static self-gravitational fluids can be described via uniform energy density plus the change induced by the non-uniform distribution of energy density as

$$m(r) = \frac{4\pi}{3}r^3\widetilde{\varepsilon} - \frac{4\pi}{3}\int_0^r [\widetilde{\varepsilon}(u)]' u^3 du + \frac{s^2}{2r} + \frac{1}{2}\int_0^r \frac{s^2}{u^2}du. \tag{39}$$

Next, using Eqs. (7)–(9), we get

$$m(r) = m_0(r) + \alpha m_\Theta(r), \tag{40}$$

where

$$m_0(r) = \frac{4\pi}{3}r^3\varepsilon - \frac{4\pi}{3}\int_0^r [\varepsilon(u)]' u^3 du + \frac{s^2}{2r} + \frac{1}{2}\int_0^r \frac{s^2}{u^2}du, \tag{41}$$

$$m_\Theta(r) = \frac{4\pi}{3}r^3\varepsilon^\Theta - \frac{4\pi}{3}\int_0^r \left[\varepsilon^\Theta(u)\right]' u^3 du. \tag{42}$$

Here, m_0 and m_Θ are denotes the masses associated with Einstein–Maxwell system and the Θ-gravitational sector, respectively. Furthermore, the Tolman mass function, corresponding to the slowly evolving charged astrophysical configurations with spherical symmetry, can be defined as [70]

$$m_T = 4\pi\int_0^{r_\Sigma} u^2 e^{(\nu+\lambda)/2}\Big(\widetilde{T}_0^{\ 0} + S_0^{\ 0} - \widetilde{T}_1^{\ 1} - S_1^{\ 1} - 2\widetilde{T}_2^{\ 2} - 2S_2^{\ 2}\Big)du. \tag{43}$$

The mass m_T signifies the total energy content of the compact fluid system, which can also be expressed as

$$m_T = e^{(\nu+\lambda)/2}\left(m(r) + 4\pi r^3\widetilde{P}_r - \frac{s^2}{2r}\right), \tag{44}$$

or alternatively

$$m_T = [m_T(r)]_\Sigma\left(\frac{r}{r_\Sigma}\right)^3 - r^3\int_r^{r_\Sigma}\left[\frac{4\pi}{u^4}\int_0^{r_\Sigma}\left([\varepsilon(u)] + \frac{s^2}{8\pi r^4}\right)' \times u^3 du - \frac{8\pi}{u}\left(\Delta^{eff} - \frac{s^2}{4\pi r^4}\right)\right]e^{(\nu+\lambda)/2}du. \tag{45}$$

The above expression can be represented in terms of Weyl scalar as

$$m_T = [m_T(r)]_\Sigma \left(\frac{r}{r_\Sigma}\right)^3 + r^3 \int_r^{r_\Sigma} \frac{1}{u} e^{(\nu+\lambda)/2} \times \left[4\pi\left(\Delta^{eff} - \frac{s^2}{4\pi r^4}\right) + E\right] du. \tag{46}$$

In terms of the structure scalar Y_{TF}, we can rewrite m_T as

$$m_T = \left(\frac{r}{R}\right)^3 M_T + r^3 \int_r^R \frac{e^{(\nu+\lambda)/2}}{u} \widetilde{Y}_{TF} du, \tag{47}$$

where M_T denotes the overall Tolman mass of self-gravitational fluid with spherically symmetric configuration of radius R. To establish a physically viable and complete solution for the self-gravitational compact configuration, it is essential to smoothly satisfy the junction constraints across the boundary surface Σ of the astrophysical configuration with the familiar Reissner–Nordström metric, as defined by

$$ds^2 = g_{\mu\eta} dx^\mu dx^\eta, \quad g_{\mu\eta} = \text{diag}\left[\left(1 - \frac{2M}{r} + \frac{q^2}{r^2}\right), -\left(1 - \frac{2M}{r} + \frac{q^2}{r^2}\right)^{-1}, - r^2, -r^2 \sin^2\theta\right]. \tag{48}$$

Here, M and q encode the total relativistic mass and charge corresponding to the astrophysical compact distribution, respectively. The continuity of the first and second fundamental forms across Σ, gives

$$e^{\nu_\Sigma} = \left(1 - \frac{2M}{r_\Sigma} + \frac{q^2}{r_\Sigma^2}\right), \tag{49}$$

$$e^{-\lambda_\Sigma} = \left(1 - \frac{2M}{r_\Sigma} + \frac{q^2}{r_\Sigma^2}\right), \tag{50}$$

$$P_r(r_\Sigma) = 0, \tag{51}$$

$$s(r_\Sigma) = q. \tag{52}$$

The above expressions describe the necessary and sufficient conditions for the smooth joining of both the geometries.

4 Complexity of self-gravitational fluid spheres

This section explores the key ingredients for establishing the notion of complexity within the framework of static, anisotropic spherical fluid configurations as discussed by Herrera [1]. The novelty of this idea lies in one of its primary features: assigning zero complexity to systems that are isotropic in terms of pressure and uniform in terms of density. In this scheme, the complexity of anisotropic fluids spheres is determined by a scalar function, which is associated with the family of variables so-called structure scalars. The formulation of these scalar terms is primarily linked to the well-known scheme of orthogonal decomposition of tensorial quantity $R_{\mu\eta\gamma\delta}$ (known as Riemann tensor). These scalars are important for exploring the structural features inherent to the time-independent as well as time-dependent self-gravitational fluid spheres. Here, we will provide a concise overview of how they are obtained. For spherically symmetric compact fluid sources, the Weyl tensor ($C_{\mu\eta\gamma\delta}$) is defined in terms of its electric part ($E_{\mu\eta}$) only since the magnetic part disappears as a result of spherical symmetry.

$$E_{\mu\eta} = C_{\mu\eta\gamma\delta} U^\eta U^\delta, \tag{53}$$

where U^μ denotes the four velocity for the given fluid configuration. The above expression can be rewritten in terms of Weyl scalar E, unit four vector $K_\mu = \left(0, e^{-\lambda/2}, 0, 0\right)$ and the projection tensor $h_{\mu\eta}$ as

$$E_{\mu\eta} = E\left(K_\mu K_\eta - \frac{1}{2} h_{\mu\eta}\right), \tag{54}$$

where

$$h_{\mu\eta} = g_{\mu\eta} + U_\mu U_\eta \quad \text{and} \quad E = \frac{1}{4}\left[\frac{2}{r^2}(e^{-\lambda} - 1) + \frac{1}{r}(\lambda' - \nu') - \frac{\nu'}{2}\left(\nu' - \lambda'\right) - \nu''\right] e^{-\lambda}. \tag{55}$$

Herrera and his coworkers described that $R_{\mu\eta\gamma\delta}$ can be written using the following tensorial terms (for details see [1,65])

$$Y_{\mu\eta} = R_{\mu\eta\gamma\delta} U^\eta U^\delta, \tag{56}$$

$$X_{\mu\eta} =^* R^*_{\mu\eta\gamma\delta} U^\eta U^\delta = \frac{1}{2} \xi_{\mu\eta}{}^{\varsigma\upsilon} R^*_{\varsigma\upsilon\gamma\delta} U^\eta U^\delta, \quad \text{with} \quad R^*_{\mu\eta\gamma\delta} = \frac{1}{2} \xi_{\varsigma\upsilon\gamma\delta} R_{\gamma\delta}{}^{\varsigma\upsilon}. \tag{57}$$

The terms $Y_{\mu\eta}$ and $X_{\mu\eta}$ can be represented through four structure scalars $\{Y_{TF}, Y_T, X_{TF}, X_T\}$ as

$$Y_{\mu\eta} = \left(K_\mu K_\eta - \frac{1}{3} h_{\mu\eta}\right) Y_{TF} + \frac{1}{3} h_{\mu\eta} Y_T, \tag{58}$$

$$X_{\mu\eta} = \left(K_\mu K_\eta - \frac{1}{3} h_{\mu\eta}\right) X_{TF} + \frac{1}{3} h_{\mu\eta} X_T. \tag{59}$$

Then, combining the Einstein–Maxwell equations (27)–(29) with Weyl scalar E, we obtain the expressions for the electrically charged scalars $\left\{\widetilde{Y}_{TF}, \widetilde{Y}_T, \widetilde{X}_{TF}, \widetilde{X}_T\right\}$ as [65]

$$\widetilde{Y}_{TF} = 4\pi\Delta^{eff} + E - \frac{s^2}{r^4} = 8\Delta^{eff} - \frac{2s^2}{r^4} - \frac{4\pi}{r^3}\int_0^r \left(\widetilde{\varepsilon} + \frac{s^2}{8\pi r^4}\right) u^3 du, \tag{60}$$

$$\widetilde{Y}_T = 4\pi(\widetilde{\varepsilon} + 3\widetilde{P}_r - 2\Delta^{eff}) + \frac{s^2}{r^4}, \tag{61}$$

$$\widetilde{X}_{TF} = 4\pi\Delta^{eff} - E - \frac{s^2}{r^4} = \frac{4\pi}{r^3}\int_0^r \left(\widetilde{\varepsilon} + \frac{s^2}{8\pi r^4}\right) u^3 du, \tag{62}$$

$$\widetilde{X}_T = 8\pi\left(\widetilde{\varepsilon} + \frac{s^2}{8\pi r^4}\right). \tag{63}$$

Now, we can clearly specify the effective structure scalars appearing in Eqs. (60)–(63) as

$$\widetilde{Y}_{TF} \equiv Y_{TF} + Y^{\Theta}_{TF}, \tag{64}$$

$$\widetilde{Y}_T \equiv Y_T + Y^{\Theta}_T, \tag{65}$$

$$\widetilde{X}_{TF} \equiv X_{TF} + X^{\Theta}_{TF}, \tag{66}$$

$$\widetilde{X}_T \equiv X_T + X^{\Theta}_T. \tag{67}$$

Now, we will construct the solutions corresponding to the gravitational systems (27)–(29) and (32)–(34). The solution of the system of DEs (27)–(29) requires two conditions due to the presence of the five unknown variables $\{\omega, \sigma, \varepsilon, P, s\}$ within that system. However, the solution of the $\Theta_{\mu\eta}$ fluid requires the obtention of the solution for the system (32)–(34) corresponding to the $T_{\mu\eta}$ fluid source. In this context, we employ two conditions: (i) a suitable model for the metric potential and (ii) Embedding Class I condition. Any metric describes an Embedding Class I metric if it obeys the Karmarkar condition, which is defined as

$$R_{1212}R_{3030} = R_{1220}R_{1330}R_{1010}R_{2323}, \tag{68}$$

such that $R_{2323} \neq 0$. For the spherically symmetric metric ansatz (31), the above expression turns out to be

$$\frac{2\omega''}{\omega'} + \omega' = -\frac{\sigma'}{\sigma(1-\sigma)}, \quad \sigma \neq 0, \tag{69}$$

whose integration reads

$$\omega(r) = 2\ln\left[C_1 + C_2\int\left(\frac{1-\sigma}{\sigma}\right)^{1/2} dr\right], \tag{70}$$

with C_1 and C_2 being the integration constants. The above expression describe a relationship between the geometric variables $\{\omega, \sigma\}$. In the next section, we will employ two different ansatzes (Tolman and Buchdahl) to examine the influence of complexity using the structure scalars associated with the density and pressure of the electrically charged self-gravitational compact configurations.

4.1 Minimally deformed complexity-free Buchdahl Ansatz

Let us consider the Buchdhal ansatz, which is expressed as

$$\sigma(r) = \frac{1 + Ar^2}{1 + Br^2}. \tag{71}$$

Here, A and B denote integration constants with units $[length^{-2}]$. This metric ansatz has been extensively used in deriving the solutions of spherically symmetric, self-gravitational fluid configurations [71–74]. Now, using the Buchdhal ansatz in (72), we obtain

$$\omega(r) = 2\ln[C + D\sqrt{1 + Ar^2}], \tag{72}$$

where $C = C_1$ and $D = \frac{1}{A}(B - A)^{1/2}C_2$. Then, using the metric potentials $\{\sigma, \omega\}$ in the system of DEs (27)–(29), the physical variables $\{s, P, \varepsilon\}$ read

$$\frac{s^2}{r^4} = \frac{Br^2\left[-2DA^2r^2 + B(C + D\varphi) + A\left(-C\varphi + D(-2 + Br^2)\right)\right]}{2\varphi\left(1 + Br^2\right)^2(C + D\varphi)}, \tag{73}$$

$$8\pi P = \frac{\left[-2DA^2r^2 + B(2 + 3Br^2)(C + D\varphi) + AC\varphi(2 + 3Br^2) - D(2 + 2Br^2 + 3B^2r^4)\right]}{2\varphi\left(1 + Br^2\right)^2(C + D\varphi)}, \tag{74}$$

$$8\pi\varepsilon = \frac{\left[-2DA^2r^2(3 + 2Br^2) + 3B(2 + Br^2)(C + D\varphi) + A\left(-3D\varphi(2 + Br^2) + D(-6 + 2Br^2 + 3B^2r^2)\right)\right]}{2\varphi\left(1 + Br^2\right)^2(C + D\varphi)}, \tag{75}$$

with $\varphi = \sqrt{1+Ar^2}$. Next, we proceed to construct the solution corresponding to the additional fluid $\Theta_{\mu\eta}$, which is influenced by $\mathcal{G}(r)$. To solve this, we impose the complexity-free condition on the effective gravitational source $T_{\mu\eta}$, that is $\widetilde{T}_{TF} = 0$, with $Y_{TF} \neq 0$. Then, Eq. (60) takes the following form

$$\widetilde{Y}_{TF} = 4\pi\,\Delta^{eff} + E - \frac{s^2}{r^4} \equiv Y_{TF} + Y^{\Theta}_{TF} = 0, \tag{76}$$

where Y_{TF} is determined by the seed variables $\{\varepsilon, P, s\}$, therefore

$$\widetilde{Y}_{TF} = \frac{\left[\nu'(2 - r\nu' + r\lambda') - 2r\nu''\right]}{4re^{\lambda}} - \frac{s^2}{r^4}, \tag{77}$$

which is defined as

$$\widetilde{Y}_{TF} = \frac{\left[\left(A^2Dr^2(5C+4D\varphi) - B(2CD + C^2\varphi + D^2\varphi) - A\left(-C^2\varphi + D^2\varphi(-4+Br^2) + CD(-5+2Br^2)\right)\right)\right]}{2\varphi\left(Br^2\right)^{-1}\left(1+Br^2\right)^2(C+D\varphi)^2}. \tag{78}$$

Also, for the Eq. (76), we obtain

$$\omega'\mathcal{G}' + \left[2\omega'' + \left(\omega' - \frac{2}{r}\right)\omega'\right]\mathcal{G} - 4Y_{TF} = 0. \tag{79}$$

Then, the combination of the metric potentials $\{\sigma, \omega\}$ with Y_{TF} produces the following form of the deformation function

$$\begin{aligned}\mathcal{G}(r) = L(1+Ar^2) - \frac{B(1+Ar^2)}{2A(A-B)D} \\ \times\left[\frac{\left(3A^2+(B-4)B+B^2\right)D + \left(A^2 - A(B-2)B + B^2\right)C\varphi}{B(1+Br^2)}\right. \\ - \frac{A\left(A^2 - A(B-2)B + B^2\right)C}{B^{3/2}\sqrt{B-A}}\tanh^{-1}\left(\frac{\varphi\sqrt{B}}{\sqrt{B-A}}\right) \\ \left. + \frac{A\left(A(B-1)+B\right)}{(A-B)}\ln\left(\frac{1+Ar^2}{1+Br^2}\right)\right],\end{aligned} \tag{80}$$

where L is constant of integration. To determine the value of L, we employ the physically acceptable condition for the metric potential $e^{-\lambda(r)} = \sigma(r) + \alpha\mathcal{G}(r)$, which requires it to be equal to unity at the core, that is $e^{-\lambda(r)} = 1$. This conditions implies that $\mathcal{G}(0) = 0$, which gives

$$\begin{aligned}L = \frac{\left(3A^2+(B-A)B+B^2\right)D + \left(A^2 - AB(B-2) + B^2\right)C}{2A(A-B)D} \\ - \frac{AC\left(A^2 + AB(B-4) + B^2\right)}{\sqrt{B(B-A)}} \\ \times\tanh^{-1}\left(\sqrt{\frac{B}{B-A}}\right).\end{aligned} \tag{81}$$

Then, the transformation (26) in combination with Eq. (80) defines the new form of radial metric potential $e^{-\lambda(r)}$. Now, the physical variables $\left\{\varepsilon^{\Theta}, P^{\Theta}_r, P^{\Theta}_{\perp}\right\}$ associated with Θ-gravitational sector read

$$\begin{aligned}8\pi\varepsilon^{\Theta} = -\frac{\alpha}{r^2}\left[r^2\left\{\frac{B\left(A^3Cr^4 - B(C+D\varphi) + A^2r^2((B-1)C+3D\varphi) - A\left((B-4)D\varphi + C\left(2+B(r^2-1)\right)\right)\right)}{AD\varphi(1+Br^2)^2}\right.\right. \\ \left.\left. + 2AL - \chi^{(1)}\right\} + L(1+Ar^2) - \frac{\chi^{(1)}}{2A(1+Ar^2)}\right],\end{aligned} \tag{82}$$

$$8\pi P^{\Theta}_r = \frac{\alpha}{2}\left(\frac{D+3ADr^2+C\varphi}{r^2(D+ADr^2+C\varphi)}\right)(1+Ar^2)(2L-\chi^{(1)}),$$

$$8\pi P^{\Theta}_{\perp} = \frac{\alpha}{2}\left[r^2\left(\frac{B\left(A^3Cr^4 - B(C+D\varphi) + A^2r^2((B-1)C+3D\varphi) - A\left((B-4)D\varphi + C\left(2+B(r^2-1)\right)\right)\right)}{AD\varphi(1+Br^2)^2}\right.\right. \tag{83}$$

$$\left.\left. + 2AL - \chi^{(1)}\right)\left(\frac{D+2ADr^2+\varphi C}{r(D+ADr^2+\varphi C)}\right)(-r) + \frac{AD(2+Ar^2)}{\varphi(C+D\varphi)}\left(2L-\chi^{(1)}\right)\right] \tag{84}$$

where the value of $\chi^{(1)}$ is given in Appendix. The corresponding new radial metric potential will modify the structure scalar Y_{TF} (defined in (78)) to

$$\widetilde{Y}_{TF} = -\Big[Br^2\Big(-B(2CD+C^2\varphi+D^2\varphi)(-1+\alpha) +A^3CD\alpha r^4+A\Big(CD(-5-Br^2(-2+\alpha)+2\alpha) +C^2\varphi(-1+(-2+\alpha)\alpha)+C^2\varphi(-1+(-2+B)\alpha) +D^2\varphi(-4+Br^2+4\alpha-B\alpha)\Big) +A^2r^2(C^2\varphi\alpha+D^2\varphi(-4+3\alpha)+CD(-5+(2+B)\alpha))\Big)\Big] /\Big(2\varphi\left(1+Br^2\right)^2(C+D\varphi)^2\Big). \tag{85}$$

The above relation can be used to determine the impact of decoupling parameter α on the structure scalar $\widetilde{Y}_{TF}$, which is defined as a variable for defining the complexity of the system.

$$\widetilde{X}_{TF} = \frac{1}{2r^2}\Bigg[-2+\frac{Br^4(2A^2Dr^2-B(C+D\varphi)+A(C\varphi+D(2-Br^2))}{2\alpha(1+Br^2)^2(C+D\varphi)} +(1+Ar^2)\left\{\frac{2}{1+Br^2}+\alpha\left(2L-\chi^{(1)}\right)\right\} -r^2\left\{\alpha\left(2AL+\frac{B\left(A^3Cr^4-B\left(C+D\varphi\right)+A^2r^2\left((B-1)C+3D\varphi\right)-A\left((B-4)D\varphi+C\left(2+B(r^2-1)\right)\right)\right)}{AD\varphi(1+Br^2)^2} -\chi^{(1)}\right)+\frac{2A}{1+Br^2}-\frac{2B(1+Ar^2)}{(1+Br^2)^2}\right\}\Bigg], \tag{86}$$

$$\widetilde{Y}_T = \Big[-B(D+L\varphi)(8+3Br^2+4\alpha) -2A^2Dr^2\left(-3+B^2r^4\alpha+Br^2(1+4\alpha)\right) +A\Big(C\varphi\left(8+Br^2(3-8\alpha)-4\alpha B^2r^4\right) +D\left(6+B^2r^4(-3+2\alpha)-2Br^2(5+4\alpha)\right)\Big)\Big] \Big/\Big(2\varphi\left(1+Br^2\right)^2(C+D\varphi)^2\Big), \tag{87}$$

$$\widetilde{X}_T = \Big[-B(D+C\varphi)\left(Br^2(-2+\alpha)+3(-1+\alpha)\right) -A^2Nr^2\left(3+3\alpha B^2r^4+Br^2(3+5\alpha)\right) -2ADB^2r^4(-1+2\alpha)-A\Big(D\left(3+8\alpha Br^2\right) +C\varphi\left(3+8\alpha Br^2+2B^2r^4(-1+2\alpha)\right) +C\varphi\left(3+3\alpha B^2r^4+Br^2(2+5\alpha)\right)\Big)\Big]\Big/2\varphi \times\Big(\left(1+Br^2\right)^2(C+D\varphi)^2\Big). \tag{88}$$

4.2 Minimally deformed complexity-free Tolman Ansatz

This subsection probes the construction of electrically charged, complexity-free self-gravitational model under radial metric transformation (minimal geometric deformation) by assuming the well-known Tolman model

$$\sigma(r) = \frac{1}{1+Ar^2+Br^4}. \tag{89}$$

Here, A and B are integration constants with units $[length^{-2}]$ and $[length^{-4}]$, respectively. Then, under the Tolman model, the embedding Class I conditions reads

$$\omega(r) = 2\ln\left[\left(C+D\left(A+Br^2\right)^{3/2}\right)\right], \tag{90}$$

with $C = C_1$ and $D = \frac{C_2}{3B}$. Then, the physical variables $\{s, P, \varepsilon\}$ turn out to be

$$\frac{s^2}{r^4} = \frac{r^2\left(A^2D-3BD+2ABDr^2+B^2Dr^4+C\sqrt{A+Br^2}\right)\left(A^2+2ABr^2+B(-1+Br^4)\right)}{\sqrt{A+Br^2}(1+Ar^2+Br^4)^2\left(C+D(A+Br^2)^{3/2}\right)}, \tag{91}$$

$$
\begin{aligned}
8\pi P = &\Big[-r^2\Big(A^2D - 3BD + 2ABDr^2 + B^2Dr^4 \\
&+ C\sqrt{A+Br^2}\Big) \times \Big(A^2 + 2ABr^2 + B(-1+Br^4)\Big) \\
&-6BD(A+Br^2)(1+Ar^2+Br^4)r^2 \\
&+\Big(1-(1+Ar^2+Br^4)\Big)\sqrt{A+Br^2}(1+Ar^2+Br^4) \\
&\times \Big(C + D(A+Br^2)^{3/2}\Big)\Big] \Big/ r^2\sqrt{A+Br^2}(1+Ar^2+Br^4)^2 \\
&\times \Big(C + D(A+Br^2)^{3/2}\Big), \qquad (92)
\end{aligned}
$$

$$
\begin{aligned}
8\pi\varepsilon = &\Big[\sqrt{A+Br^2}\Big(C + D\Big(A+Br^2\Big)^{3/2}\Big) \\
&\times \Big(r^2(1+Ar^2+Br^4)^2 + 2r^2(A+2Br^2) - (1+Ar^2+Br^4)\Big) \\
&+ r^2\Big(A^2D - 3BD + 2ABDr^2 + B^2Dr^4 + C\sqrt{A+Br^2}\Big) \\
&\times \Big(A^2 + 2ABr^2 + B(-1+Br^4)\Big)\Big] \Big/ r^2 \\
&\times \sqrt{A+Br^2}(1+Ar^2+Br^4)^2\Big(C + D(A+Br^2)^{3/2}\Big). \qquad (93)
\end{aligned}
$$

The corresponding complexity factor Y_{TF} takes the form

$$
\begin{aligned}
Y_{TF} = &-\Big[r^2\left(A^2 + 2ABr^2 + B\left(-1+Br^4\right)\right) \\
&\times \Big(-6BCD + \sqrt{A+Br^2}\left(C^2 + A^3D^2 + B^3D^2r^6\right) + 2B^2Dr^2 \\
&\times \Big(Cr^2 - 3D\sqrt{A+Br^2}\Big) + A^2D\Big(2C + 3BDr^2\sqrt{A+Br^2}\Big) \\
&+ABD\Big(4Cr^2 + 3D\sqrt{A+Br^2}\left(-2+Br^4\right)\Big)\Big)\Big] \\
&\Big/\Big(\sqrt{A+Br^2}(1+Ar^2+Br^4)^2\left(C + D(A+Br^2)^{3/2}\right)^2\Big). \qquad (94)
\end{aligned}
$$

Now, using the Tolman ansatz in Eq. (79), we obtain

$$
\frac{6BDr\left(2Br\mathcal{G} + (A+Br^2)\mathcal{G}'\right)}{A^2D + 2ABDr^2 + B^2Dr^4 + C\sqrt{A+Br^4}} - 4Y_{TF} = 0 \qquad (95)
$$

Then, the combination of (94) and (95) produces the deformation function for the minimally deformed Tolman model

$$
\begin{aligned}
\mathcal{G}(r) = &\frac{L}{A+Br^2} \\
&+\left(\frac{A^2D - 8BD - B^2Dr^4 + C\sqrt{A+Br^2}}{12BD(1+Ar^2+Br^4)} - \frac{\chi^{(2)}}{6BD}\right), \qquad (96)
\end{aligned}
$$

where the value of $\chi^{(2)}$ is given in Appendix. Furthermore, L is an integration constant, whose value can be found by making use of the physically viable condition: $e^{-\lambda(0)} = \sigma(0) + \alpha\mathcal{G}(0) = 1$, which implies $\mathcal{G}(0) = 0$, and thus,

$$
\begin{aligned}
L = &\frac{A}{6BD}\Bigg[\frac{(-A^2+2B)BD}{\sqrt{-A^2+4B}}\tan^{-1}\left(\frac{A+2B^2}{\sqrt{-A^2+B}}\right) \\
&+\frac{AB - B\sqrt{A^2-4B}}{2\sqrt{2}\sqrt{A-\sqrt{A^2+4B}}\sqrt{A^2-4B}} \\
&\times C\tan^{-1}\left(\frac{\sqrt{2}\sqrt{A}}{\sqrt{A-\sqrt{A^2-4B}}\sqrt{A^2-4B}}\right) \\
&-\frac{AB + B\sqrt{A^2-4B}}{2\sqrt{2}\sqrt{A+\sqrt{A^2+4B}}\sqrt{A^2-4B}} \\
&\times C\tan^{-1}\left(\frac{\sqrt{2}\sqrt{A}}{\sqrt{A+\sqrt{A^2-4B}}\sqrt{A^2-4B}}\right)\Bigg] \\
&-\frac{A\left(A^2D - 8BD + C\sqrt{A}\right)}{12BD}. \qquad (97)
\end{aligned}
$$

The physical variables associated with $\Theta_{\mu\eta}$ fluid source transform as

$$
\begin{aligned}
\varepsilon^{\Theta} = &\frac{\alpha}{12r^2(A+Br^2)^2}\Bigg[-12L(A+Br^2) - \frac{\chi^{(3)}}{BD(A+Br^2)} + 24BLr^2 + \frac{2r^2}{D}\chi^{(3)} + 2r^2 \\
&\Bigg\{\frac{\left(A^2D\sqrt{A+Br^2} + A\left(C + 2BDr^2\sqrt{A+Br^2}\right) + B\left(Cr^2 + D\sqrt{A+Br^2}(-6+Br^4)\right)\right)}{BD(1+Ar^2+Br^4)^2} \\
&\times \left(A^2 + 2ABr^2 + B(-1+Br^4)\right)\sqrt{A+Br^2}\Bigg\}\Bigg], \qquad (98)
\end{aligned}
$$

$$
\begin{aligned}
P_r^{\Theta} = &\frac{\alpha}{A+Br^2}\left(\frac{1}{r^2} + \frac{6BD\sqrt{A+Br^2}}{C + D(A+Br^2)^{3/2}}\right)\Bigg[L + \frac{(A+Br^2)\left(A^2D - 8BD - B^2Dr^4 + C\sqrt{A+Br^2}\right)}{12BD(1+Ar^2+Br^4)} \\
&-\frac{1}{24D}\Bigg\{\frac{4(A^2-2B)D}{\sqrt{-A^2+4B}}\tanh^{-1}\left(\frac{A+2B^2}{\sqrt{-A^2+B}}\right) + \frac{\sqrt{2}\sqrt{A-\sqrt{A^2-4B}}}{\sqrt{A^2-4B}}C\tanh^{-1}\left(\frac{\sqrt{2}\sqrt{A+Br^2}}{\sqrt{A-\sqrt{A^2-4B}}}\right) \\
&-\frac{\sqrt{2}\sqrt{A+\sqrt{A^2-4B}}}{\sqrt{A^2-4B}}C\tanh^{-1}\left(\frac{\sqrt{2}\sqrt{A+Br^2}}{\sqrt{A+\sqrt{A^2-4B}}}\right) + \ln(1+Ar^2+Br^4)\Bigg\}\Bigg] \Big/ \left(A+Br^4\right), \qquad (99)
\end{aligned}
$$

$$P_{\perp}^{\Theta}=3\alpha BD(2A+3Br^2)\Bigg[L+\frac{(A+Br^2)\left(A^2D-8BD-B^2Dr^4+C\sqrt{A+Br^2}\right)}{12BD(1+Ar^2+Br^4)}-\frac{1}{24D}$$
$$\times\left\{\frac{4(A^2-2B)D}{\sqrt{-A^2+4B}}\tanh^{-1}\left(\frac{A+2B^2}{\sqrt{-A^2+B}}\right)\quad+\frac{\sqrt{2}\sqrt{A-\sqrt{A^2-4B}}}{\sqrt{A^2-4B}}C\tanh^{-1}\left(\frac{\sqrt{2}\sqrt{A+Br^2}}{\sqrt{A-\sqrt{A^2-4B}}}\right)\right.$$
$$\left.-\frac{\sqrt{2}\sqrt{A+\sqrt{A^2-4B}}}{\sqrt{A^2-4B}}C\tanh^{-1}\left(\frac{\sqrt{2}\sqrt{A+Br^2}}{\sqrt{A+\sqrt{A^2-4B}}}\right)\right\}\Bigg]\Big/\left((A+Br^2)\left(A^2D+2ABDr^2+B^2Dr^4\ +\ C\sqrt{A+Br^2}\right)\right)$$
$$-\frac{\alpha r}{6(A+Br^2)^2}\left(\frac{1}{r}+\frac{3BDr\sqrt{A+Br^2}}{\left(C+D(A+Br^2)^{3/2}\right)}\right)$$
$$\times\left\{-12BL-\frac{\left(A^2D\sqrt{A+Br^2}+A\left(C+2BDr^2\sqrt{A+Br^2}\right)+B\left(Cr^2+D\sqrt{A+Br^2}(-6+Br^4)\right)\right)}{BD(1+Ar^2+Br^4)^2}\right.$$
$$\left.\times\left(A^2+2ABr^2+B(-1+Br^4)\right)\sqrt{A+Br^2}+\frac{\chi^{(3)}}{D}\right\},\tag{100}$$

where the value of $\chi^{(3)}$ is given in Appendix. Furthermore, the modified form of the complexity factor Y_{TF} for the Tolman ansatz are defined as

$$Y_{TF}=(-4+\alpha)r^2\left(A^2+2ABr^2+B(-1+Br^2)\right)$$
$$\times\left(-6BCD+C^2\sqrt{A+Br^2}+A^3D^2\sqrt{A+Br^2}\right.$$
$$+B^3D^2r^6\sqrt{A+Br^2}+2B^2Dr^2\left(Cr^2-3D\sqrt{A+Br^2}\right)$$
$$+A^2D\left(2C+3BDr^2\sqrt{A+Br^2}\right)$$
$$\left.+ABD\left(4Cr^2+3D\sqrt{A+Br^2}\left(-2+Br^4\right)\right)\right)\Big/$$
$$2\sqrt{A+Br^2}(1+Ar^2+Br^4)^2\left(C+D(A+Br^2)^{3/2}\right)^2,\tag{101}$$

$$Y_T=\frac{1}{2}\Bigg[\frac{6BD\left(2A+3Br^2\right)}{\sqrt{A+Br^2}(1+Ar^2+Br^4)^2\left(C+D(A+Br^2)^{3/2}\right)}$$
$$-\frac{6BDr^2\sqrt{A+Br^2}\left(A+2Br^2\right)}{(1+Ar^2+Br^4)^2\left(C+D(A+Br^2)^{3/2}\right)}$$
$$-\frac{4(A+2Br^2)}{\left(1+Ar^2+Br^4\right)^2}-\frac{A+Br^2}{1+Ar^2+Br^4}+2\chi^{(4)}$$
$$+3\left(-\frac{6BD\sqrt{A+Br^2}}{(1+Ar^2+Br^4)\left(C+D(A+Br^2)^{3/2}\right)}\right.$$
$$\left.+\frac{1-(1+Ar^2+Br^4)}{r^2(1+Ar^2+Br^4)}\right)$$

$$X_{TF}=\frac{A+Br^2}{(1+Ar^2+Br^4)^2}$$
$$+\frac{r^2\left(A^2D-3BD+2ABDr^2+B^2Dr^4+C\sqrt{A+Br^2}\right)}{\sqrt{A+Br^2}(1+Ar^2+Br^4)^2\left(C+D(A+Br^2)^{3/2}\right)}+\frac{1}{r^2}\left(\frac{1}{1+Ar^2+Br^4}\right.$$
$$\left.+\frac{L\alpha}{A+Br^2}+\frac{\alpha\left(A^2D-8DB-B^2Dr^4+C\sqrt{A+Br^2}\right)}{\left(1+Ar^2+Br^4\right)^2}\right)-\frac{\alpha\chi^{(2)}}{24Dr^2(A+Br^2)}-\frac{\alpha}{12(A+Br^2)^2}$$
$$\times\left\{-12BL-\frac{\left(A^2D\sqrt{A+Br^2}+A\left(C+2BDr^2\sqrt{A+Br^2}\right)+B\left(Cr^2+D\sqrt{A+Br^2}(-6+Br^4)\right)\right)}{BD(1+Ar^2+Br^4)^2}\right.$$
$$\left.\times\left(A^2+2ABr^2+B(-1+Br^4)\right)\sqrt{A+Br^2}+\frac{\chi^{(3)}}{D}\right\},\tag{102}$$

$$+\frac{6\alpha BD(2A+3Br^2)\chi^{(5)}}{(A+Br^2)\left(A^2D+2ABDr^2+B^2Dr^4+C\sqrt{A+Br^2}\right)}$$
$$+\frac{\alpha}{A+Br^2}\left(\frac{1}{r^2}+\frac{6BD\sqrt{A+Br^2}}{\left(C+D(A+Br^2)^{3/2}\right)}\right)\chi^{(5)}$$
$$+\frac{\alpha}{24r^2}\left(\frac{48BLr^2}{(A+Br^2)^2}-\frac{24L}{A+Br^2}+\frac{8BDr^4-\frac{2Cr^4}{\sqrt{A+Br^2}}}{D+ADr^2+BDr^4}\right.$$
$$-\frac{4r^2(A+2Br^2)\chi^{(6)}}{BD(1+Ar^2+Br^4)^2}+\frac{2\chi^{(6)}}{BD(1+Ar^2+Br^4)}$$
$$+\frac{4(A^2-2B)D}{\sqrt{-A^2+4B}}\tan^{-1}\left(\frac{A+2B^2}{\sqrt{-A^2+B}(A+Br^2)}\right)$$
$$+\frac{\sqrt{2}\sqrt{A-\sqrt{A^2-4B}}}{D(A+Br^2)\sqrt{A^2-4B}}C\tanh^{-1}$$
$$\times\left(\frac{\sqrt{2}\sqrt{A+Br^2}}{D(A+Br^2)\sqrt{A-\sqrt{A^2-4B}}}\right)+\frac{\ln(1+Ar^2+Br^4)}{A+Br^2}$$
$$-\frac{\sqrt{2}\sqrt{A+\sqrt{A^2-4B}}}{D(A+Br^2)\sqrt{A^2-4B}}C\tanh^{-1}\left(\frac{\sqrt{2}\sqrt{A+Br^2}}{\sqrt{A+\sqrt{A^2-4B}}}\right)$$
$$+\frac{2Br^2\chi^{(5)}}{D(A+Br^2)^2}+2r^2\left(AC+BCr^2+4A^2D\sqrt{A+Br^2}\right.$$
$$\left.\left.-4BD\sqrt{A+Br^2}+4ABDr^2\sqrt{A+Br^2}\right)\Big/\right.$$
$$\left.D(A+Br^2)^{3/2}(1+Ar^2+Br^4)\right)$$
$$\left.-\frac{\alpha r}{6(A+Br^2)}\left(\frac{1}{r}+\frac{3BDr\sqrt{A+Br^2}}{\left(C+D(A+Br^2)^{3/2}\right)}\right)+\frac{\chi^{(3)}}{D}\right], \tag{103}$$

$$X_T=\frac{2(A+2Br^2)}{(1+Ar^2Br^4)^2}+\frac{A+Br^2}{1+Ar^2Br^4}+2\chi^{(4)}+\frac{\alpha}{24r^2}$$
$$\left(\frac{48BLr^2}{(A+Br^2)^2}-\frac{24L}{A+Br^2}+\frac{8BDr^4-\frac{2Cr^4}{\sqrt{A+Br^2}}}{D+ADr^2+BDr^4}\right.$$
$$-\frac{4r^2(A+2Br^2)\chi^{(6)}}{BD(1+Ar^2+Br^4)^2}+\frac{2\chi^{(6)}}{BD(1+Ar^2+Br^4)}$$
$$+\frac{4(A^2-2B)D}{\sqrt{-A^2+4B}}\tan^{-1}\left(\frac{A+2B^2}{\sqrt{-A^2+B}(A+Br^2)}\right)$$
$$+\frac{\sqrt{2}\sqrt{A-\sqrt{A^2-4B}}}{D(A+Br^2)\sqrt{A^2-4B}}$$
$$C\tanh^{-1}\left(\frac{\sqrt{2}\sqrt{A+Br^2}}{D(A+Br^2)\sqrt{A-\sqrt{A^2-4B}}}\right)$$
$$+\frac{\ln(1+Ar^2+Br^4)}{A+Br^2}$$
$$-\frac{\sqrt{2}\sqrt{A+\sqrt{A^2-4B}}}{D(A+Br^2)\sqrt{A^2-4B}}$$
$$C\tanh^{-1}\left(\frac{\sqrt{2}\sqrt{A+Br^2}}{\sqrt{A+\sqrt{A^2-4B}}}\right)+\frac{2Br^2\chi^{(5)}}{D(A+Br^2)^2}\Bigg). \tag{104}$$

5 Physical analysis

Now, we will discuss the physical viability of the electrically charged stellar solutions presented for both metric ansatzes (i.e., Buchdahl and Tolman models) under the radial metric deformation approach. We will analyze the behaviors of the matter variables and the structure scalars for the considered models that satisfy the condition $Y_{TF}=0$ by conducting a detailed graphical analysis.

5.1 First solution (Buchdahl model with $\widetilde{Y}_{TF}=0$)

The behaviors of the sets of effective fluid variables $\{\widetilde{\varepsilon},\widetilde{P}_r\}$, $\{\widetilde{P}_\perp,\Delta^{eff}\}$, and the sets of structure scalars $\{\widetilde{Y}_{TF},\widetilde{X}_{TF}\}$, $\{\widetilde{Y}_T,\widetilde{X}_T\}$ within the range $0\leq\alpha\leq 1$ versus the radial coordinate r are displayed in Figs. 1, 2, 3 and 4, respectively. Figure 1 indicates that the energy density ε (left panel) and the radial pressure $\widetilde{P}_r$ (right panel) are positive within the interior of the stellar configuration. However, both $\widetilde{\varepsilon}$ and $\widetilde{P}_r$ peak at the stellar center, after which they monotonically decrease towards the stellar surface. We noticed that the stress components increase as the value of α increases. We observe that the $\Delta^{eff}=0$ at the core and increases gradually towards the surface, reaching its peak at the surface. Moreover, the factor Δ^{eff} increases with a rise in α, as displayed in Fig. 2 (right panel). This describes how the combination of the MGD-decoupling scheme and the null-complexity constraint can be explore the anisotropies appearing in an electrically charged self-gravitational stellar solution. Furthermore, this solution is attributed to the null-complexity condition ($\widetilde{Y}_{TF}=0$), exhibiting a constant density profile under the influence of the electrically charged perfect fluid solution. This stellar solution highlights the importance of the null-complexity constraint in time-independent self-gravitational fluids, emphasizing its role in altering the state of matter configurations within such systems.

The variation of the scalar function $\widetilde{Y}_{TF}$, which is defined as the complexity factor, with different values of α is shown in Fig. 3 (left panel). By varying the α from 0 to 1, it becomes apparent that the value of $\widetilde{Y}_{TF}$ rises over a specific distance and subsequently declines towards the boundary. However, its value vanishes as the quantity α is increased. This reveals an important fact that the influence of complexity is reduced under the framework of gravitational decoupling. On the other hand, $\widetilde{Y}_{TF}$ influences thermodynamic observables, including density and pressure. Furthermore, $\widetilde{Y}_{TF}$ also influences the central values of $\{\widetilde{\varepsilon},\widetilde{P}_r\}$ because a decrease

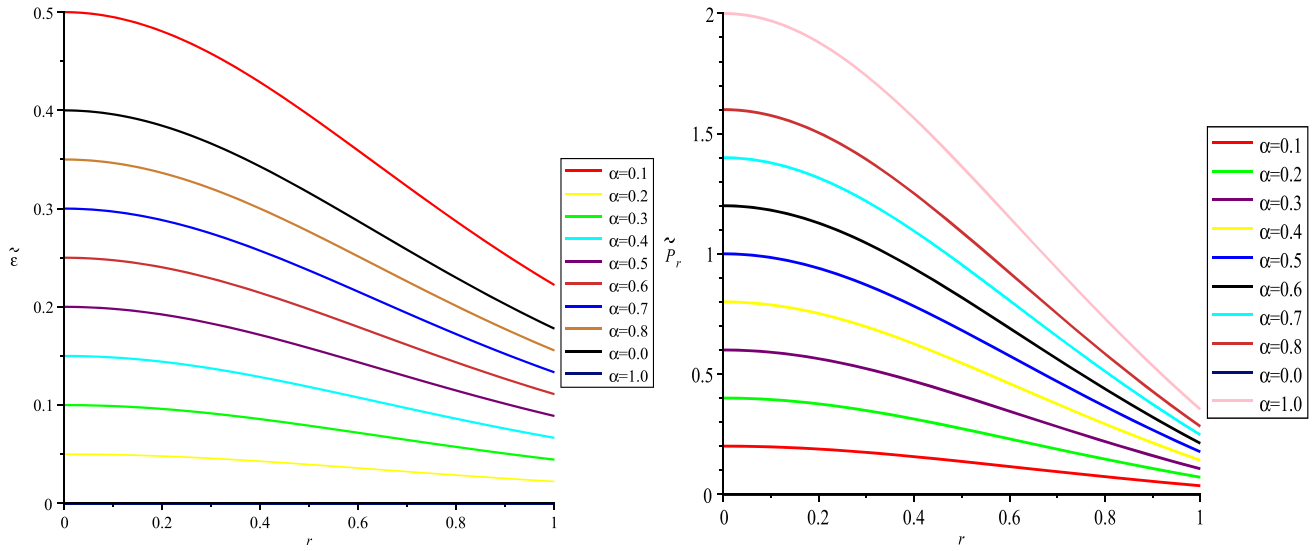

Fig. 1 Diagrammatic scheme of the total density $[\widetilde{\epsilon} \times 10^4]$ (left panel) and total radial pressure $[\widetilde{P}_r \times 10^4]$ (right panel) versus radial coordinate r corresponding to various values of decoupling constant α

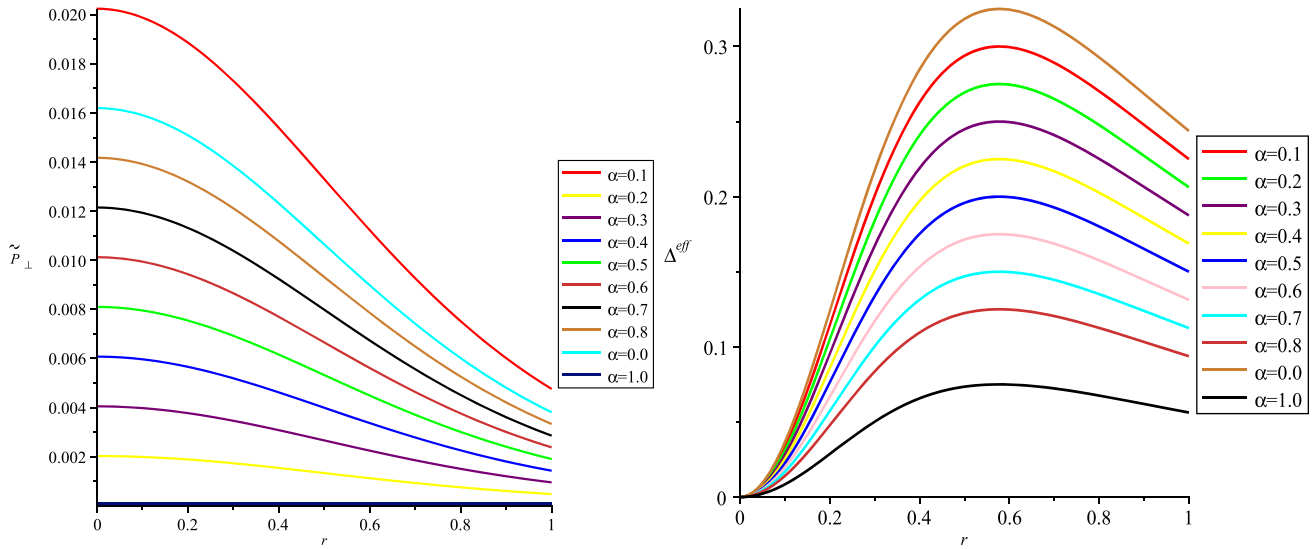

Fig. 2 Diagrammatic scheme of $[\widetilde{P}_\perp \times 10^4]$ (left panel) and $[\Delta^{eff} \times 10^4]$ (right panel) versus radial coordinate r with various values of decoupling constant α

in $\widetilde{Y}_{TF}$ leads to a decrease in these structural variables. The behavior of the obtained stellar solutions spans the entire range of values for α, representing a physically acceptable matter configuration. This is evidenced by the fulfillment of all scalar quantities, including $\widetilde{Y}_{TF}$, $\widetilde{X}_{TF}$, $\widetilde{Y}_T$, $\widetilde{X}_T$ and the homogeneous distribution of energy density.

5.2 Second solution (Tolman model with $\widetilde{Y}_{TF} = 0$)

The behavior of the four structure scalars along with the thermodynamical variables for the second stellar solution is displayed in Figs. 5, 6, 7 and 8. This presentation involves particular values of the parameter α within the range [0, 1].

Figure 5 illustrates the evolution of fluid variables, including energy density (left panel) and radial stress component (right panel). On the other hand, Fig. 6 depicts the behavior of the tangential stress component (left panel) and anisotropic factor (right panel) in relation to the radial coordinate r, considering various values of α. It is evident that the quantity $\widetilde{\varepsilon} > 0$ exhibits a uniformly decreasing profile while $\widetilde{\varepsilon} > 0$ for all allowed α-values. It is crucial to emphasize that both the principal stresses $\{\widetilde{P}_r, \widetilde{P}_\perp\}$ display monotonically decreasing profiles, while remaining positive for small values of α. Moreover, the $P_r = 0$ at a particular value of radius, indicating the boundaries of the self-gravitational configuration throughout the entire range of α at every interior point of

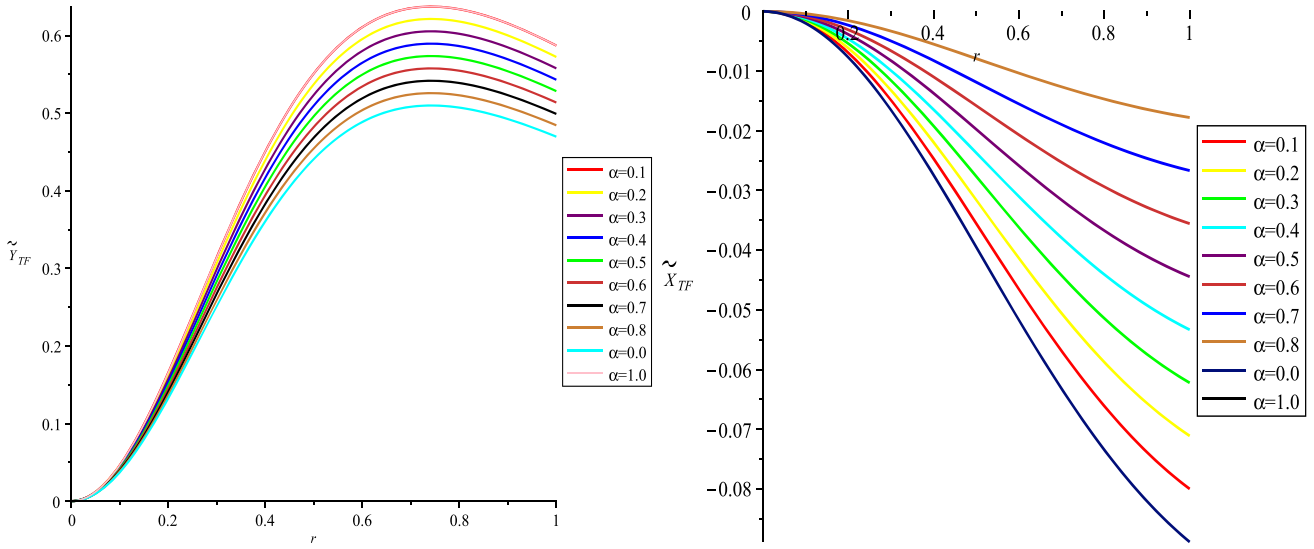

Fig. 3 Pictorial representation of the complexity factor $[\widetilde{Y}_{TF} \times 10^4]$ (left panel) and density inhomogeneity $[\widetilde{X}_{TF} \times 10^4]$ (right panel) against the radial variable r subject to different values of α

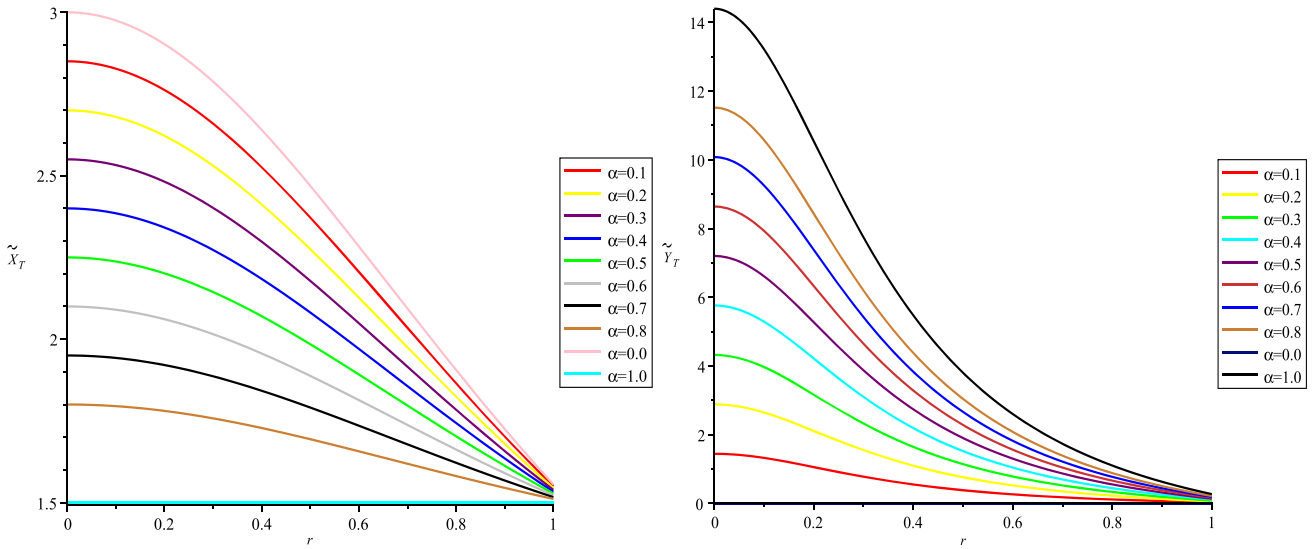

Fig. 4 Diagrammatic scheme of $[\widetilde{X}_T \times 10^4]$ (left panel) and $[\widetilde{Y}_T \times 10^4]$ (right panel) against the radial variable r with various values of the constant term α

the configuration. However, as $Y_{TF} \to 0$, there is a notable rise in stress components at every poin within the interior of the compact configuration. Figure 6 (right panel) displays that Δ^{eff} is positive across the boundary of the dense astrophysical configuration for the allowable values of α. The positive behavior of pressure anisotropy the force resulting from Δ^{eff} has a repulsive nature. By opposing the internal gravitational pull, this repulsion helps to stabilize the stellar structure. This investigation indicates that the value of the pressure aniostropy Δ^{eff} increases with an increase in the radius, effectively increasing the stability of the shell more successfully than the core regions. It is also observed that coupling MGD-decoupling with the condition $\widetilde{Y}_{TF} = 0$ reduces the factor Δ^{eff}. The profiles of the structure scalars $\{\widetilde{Y}_{TF}, \widetilde{X}_{TF}, \widetilde{X}_T, \widetilde{Y}_T\}$, which characterize physical features associated with the matter configuration for this model, is displayed in Figs. 7 and 8.

It is concluded that all these scalars exhibit profiles similar to those of the previous model, with a slight variation in $\widetilde{Y}_{TF}$. We also analyzed that the absence of the condition $\widetilde{Y}_{TF} = 0$ gives rise to a viable stellar solution. This factor significantly influences all fluid variables, resulting in a stable solution for smaller values of α. The variation of electrical charge $s(r)$ versus radial variable r for different α-values is displayed in Fig. 9. In this Fig., we observe that the magnitude of s is zero

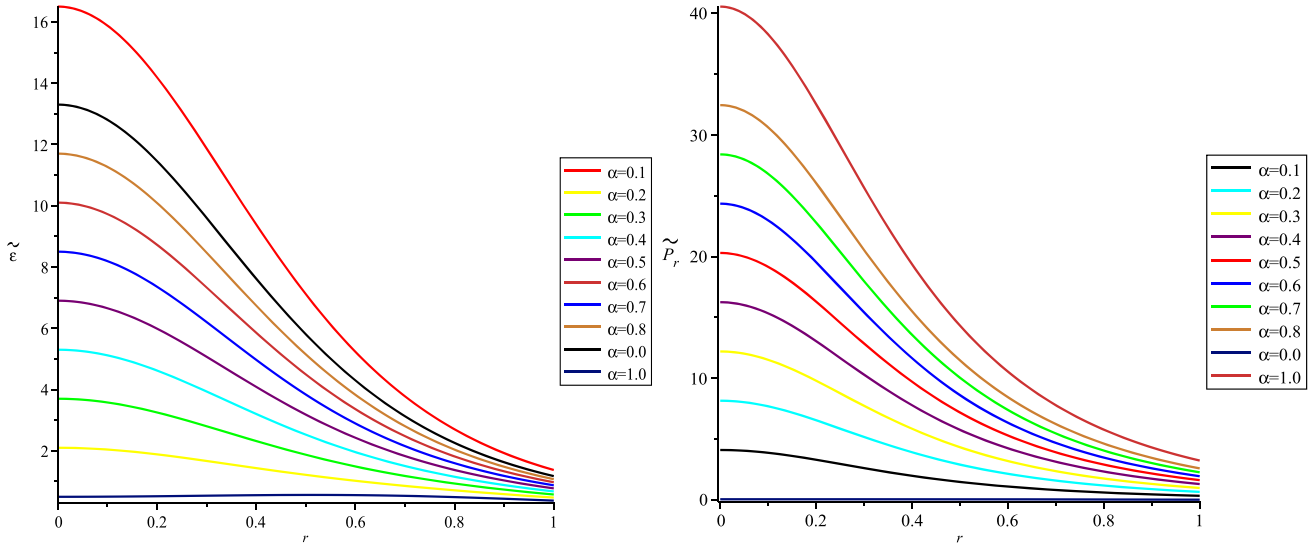

Fig. 5 The behavior of total density $[\widetilde{\epsilon} \times 10^4]$ (left panel) and total radial pressure $[\widetilde{P}_r \times 10^4]$ (right panel) against radial variable r with various α-values

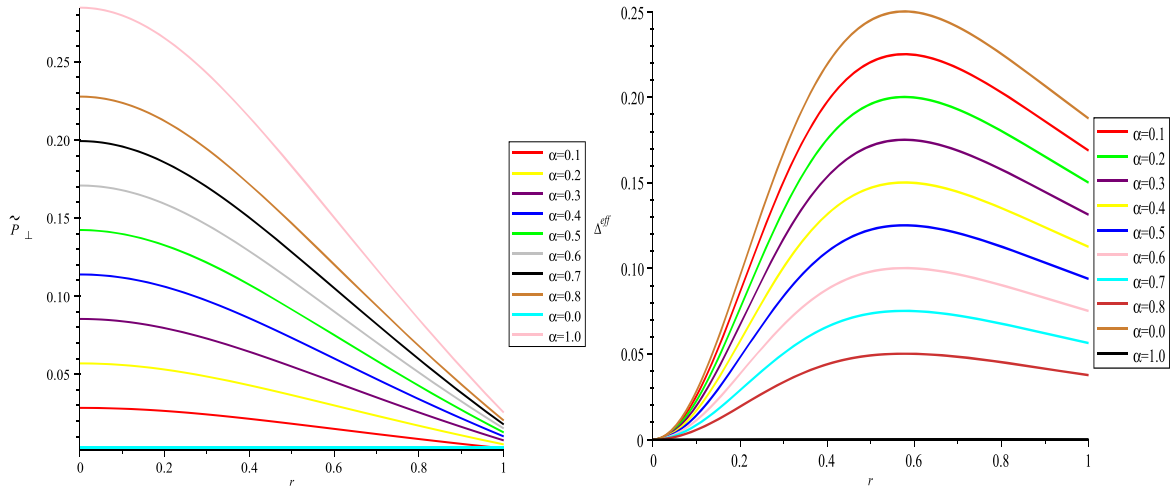

Fig. 6 The variation of $[\widetilde{P}_\perp \times 10^4]$ (left panel) and $[\Delta^{eff} \times 10^4]$ (right panel) versus radial coordinate r with various α-values

at the core and maximum at the star's surface. The amount of electric charge increases as the α-values increase.

6 Summary and discussions

It is well-established that the impact of electrical charge on the evolution of dense celestial entities, characterizing self-gravitational fluid spheres, is entirely determined by structure scalars. Motivated by the widespread applications of gravitational decoupling and structure scalars, we have established minimally deformed, self-gravitational compact solutions, with interiors modeled by electrically charged fluid distributions. We emphasize that the combination of the MGD-decoupling technique with the null-complexity condition ($\widetilde{Y}_{TF} = 0$) leads to the formation of self-gravitational systems filled with electrically charged fluid. In this respect, we employ the MGD-decoupling approach as a breakthrough tool, coupled with two metric ansatzes referred to as Buchdahl and Tolman models. This combination allows us to investigate the potential for obtaining compact distributions that represent physically viable, charged self-gravitational compact stars, characterized by a null-complexity factor. We have developed two different stellar salutations based on Buchdahl and Tolman models concerning the fluid variables $\{\widetilde{\varepsilon}, \widetilde{P}_r, \widetilde{P}_\perp, \triangle^{eff}\}$ and the structure scalars $\{\widetilde{Y}_{TF}, \widetilde{X}_{TF}, \widetilde{X}_T, \widetilde{Y}_T\}$, along with the electrically charged distribution for the self-gravitational systems through MGD-decoupling technique. This exploration involves considering specific values for the decoupling con-

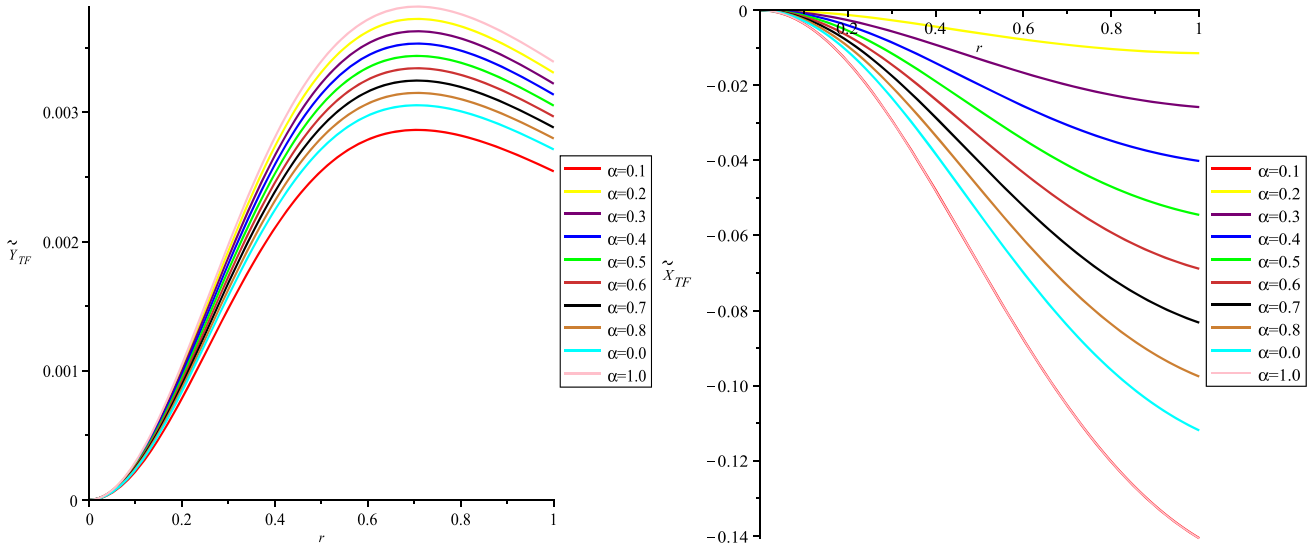

Fig. 7 Plot of the complexity factor $[\widetilde{Y}_{TF} \times 10^4]$ (left panel) and density inhomogeneity $[\widetilde{X}_{TF} \times 10^4]$ (right panel) against radial variable r subject to different values of α

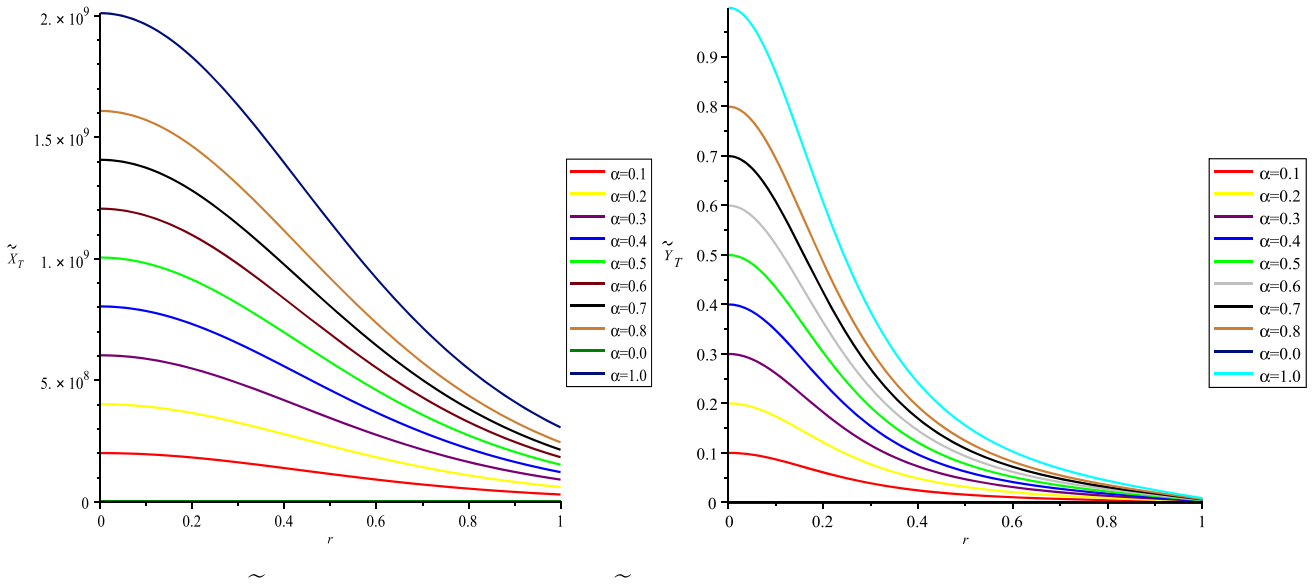

Fig. 8 The behavior of $[\widetilde{X}_T \times 10^4]$ (left panel) and $[\widetilde{Y}_T \times 10^4]$ (right panel) against radial variable r with various α-values

stant α, where $\alpha \in [0, 1]$. The effects of the Θ-gravitational source in terms of the parameter α on the thermodynamic variables are observed for both of the considered models. It is noted that both solutions behave similarly with only a minor variation in magnitude when $\widetilde{Y}_{TF} \neq 0$. However, as $\widetilde{Y}_{TF} \to 0$, the two solutions derived using the Buchdahl and Tolman stellar solutions show significant differences, particularly in the stress components and fluid's density. This implies that the scalar function $\widetilde{Y}_{TF}$, responsible for assessing the complexity of time-independent self-gravitational configurations, significantly influences the variables of the electrically charged fluid through the mechanism of MGD-decoupling.

More precisely, we have demonstrated two captivating realistic phenomena within the solution derived from the Buchdahl metric potential: the identification of a uniform density configuration and the vanishing of effective anisotropy when $\widetilde{Y}_{TF} = 0$. Moreover, we have provided some notably interesting features regarding the stress components within the solution obtained from the Tolman ansatz. We observe that as $\widetilde{Y}_{TF}$ approaches zero, there is an undesired increase in pressure at every interior point of the stellar structure. Additionally, we found that the anisotropic factor decreases due to the gravitational interactions arising from the Θ-sector subject to the null-complexity condition. It is concluded that the inclusion of $\widetilde{Y}_{TF}$ allows us to construct

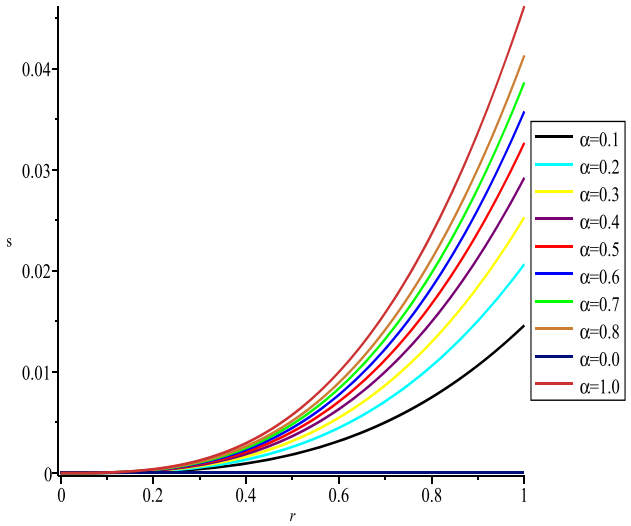

Fig. 9 Plot of electrical charge $[s(r) \times 10^4]$ against the radial variable r for various values of the constant term α

well-behaved stellar solutions. It also wields considerable influence over all fluid variables, leading to a consistent solution for smaller values of α. Consequently, we have effectively examined the relevance of scalar functions, particularly $\widetilde{Y}_{TF}$ on astrophysical compact configurations by means of MGD-decoupling technique, highly potent and useful strategy to explore realistic systems. On the other hand, the modification of the fluid variables within the compact configurations can be notably influenced by the scalar quantity $\widetilde{Y}_{TF}$ in the context of spherically symmetric, static self-gravitational distributions.

Acknowledgements This research has been funded by the Scientific Research Deanship at the University of Ha'il - Saudi Arabia through project number NT-23 015.

Data availability All data generated or analyzed during this study are included in this published article.

Code Availability Statement The manuscript has no associated code/software. [Author's comment: Not applicable.]

Funded by SCOAP[3].

Appendix

The gravitational terms arising in the Eqs. (82)–(84), (86), (96) and (98)–(104) are defined as

$$\chi^{(1)} = \frac{B}{(A-B)^2 D}$$
$$\Bigg[\frac{(A-B)\left(3A^2+AB(B-4)+B^2\right)+(A-B)\left(A^2-AB(B-2)+B^2\right)C\varphi}{B(1+Br^2)}$$
$$-AB^{-3/2}\times(A^2+A(B-4)-B^2)\sqrt{B-A}C\tanh^{-1}\left(\varphi\sqrt{\frac{B}{B-A}}\right)$$
$$+A\left(A(B-1)+B\right)C\ln\left(\frac{1+Br^2}{1+Ar^2}\right)\Bigg], \tag{105}$$

$$\chi^{(2)} = \frac{(-A^2+2B)4D}{\sqrt{-A^2+4B}}\tan^{-1}\left(\frac{A+2B^2}{\sqrt{-A^2+B}}\right)$$
$$+\frac{AB-B\sqrt{A^2-4B}}{2\sqrt{2}\sqrt{A-\sqrt{A^2+4B}}\sqrt{A^2-4B}}$$
$$\times C\tan^{-1}\left(\frac{\sqrt{2}\sqrt{A+Br^2}}{\sqrt{A-\sqrt{A^2-4B}}\sqrt{A^2-4B}}\right)$$
$$-\frac{AB+B\sqrt{A^2-4B}}{2\sqrt{2}\sqrt{A+\sqrt{A^2+4B}}\sqrt{A^2-4B}}$$
$$\times C\tan^{-1}\left(\frac{\sqrt{2}\sqrt{A+Br^2}}{\sqrt{A+\sqrt{A^2-4B}}\sqrt{A^2-4B}}\right)$$
$$+\ln\left(1+Ar^2+Br^4\right), \tag{106}$$

$$\chi^{(3)} = \Bigg[-\frac{(A+Br^2)\left(A^2D-8BD-B^2Dr^4+C\sqrt{A+Br^2}\right)}{(1+Ar^2+Br^4)}$$
$$+\Bigg\{\frac{2(A^2-2B)D}{\sqrt{-A^2+4B}}\tan^{-1}\left(\frac{A+2Br^2}{\sqrt{-A^2+B}}\right)$$
$$+\frac{\sqrt{A-\sqrt{A^2-4B}}}{\sqrt{2}\sqrt{A^2-4B}}C\tanh^{-1}\left(\frac{\sqrt{2}\sqrt{A+Br^2}}{\sqrt{A-\sqrt{A^2-4B}}}\right)$$
$$-\frac{\sqrt{A+\sqrt{A^2-4B}}}{\sqrt{2}\sqrt{A^2-4B}}C\tanh^{-1}\left(\frac{\sqrt{2}\sqrt{A+Br^2}}{\sqrt{A+\sqrt{A^2-4B}}}\right)$$
$$+ABD\ln\left(1+Ar^2+Br^4\right)\Bigg\}\Bigg], \tag{107}$$

$$\chi^{(4)} = \frac{r^2\left(A^2D-3BD+2ABDr^2+B^2Dr^4+C\sqrt{A+Br^2}\right)}{\sqrt{A+Br^2}(1+Ar^2+Br^4)^2\left(C+D(A+Br^2)^{3/2}\right)}, \tag{108}$$

$$\chi^{(5)} = \Bigg[L+\frac{(A+Br^2)\left(A^2D-8BD-B^2Dr^4+C\sqrt{A+Br^2}\right)}{12BD(1+Ar^2+Br^4)}$$
$$-\frac{1}{24D}\times\Bigg\{\frac{4(A^2-2B)D}{\sqrt{-A^2+4B}}\tanh^{-1}\left(\frac{A+2B^2}{\sqrt{-A^2+B}}\right)$$
$$+\frac{\sqrt{2}\sqrt{A-\sqrt{A^2-4B}}}{\sqrt{A^2-4B}}C\tanh^{-1}\left(\frac{\sqrt{2}\sqrt{A+Br^2}}{\sqrt{A-\sqrt{A^2-4B}}}\right)$$
$$-\frac{\sqrt{2}\sqrt{A+\sqrt{A^2-4B}}}{\sqrt{A^2-4B}}C\tanh^{-1}\left(\frac{\sqrt{2}\sqrt{A+Br^2}}{\sqrt{A+\sqrt{A^2-4B}}}\right)$$

$$+2AD\ln(1+Ar^2+Br^4)\Big\}\Big],$$

$$\chi^{(6)}=(-A^2D+8BD+B^2Dr^4-C\sqrt{A+Br^2}). \quad (109)$$

References

1. L. Herrera, Phys. Rev. D **97**, 044010 (2018)
2. S.D. Odintsov, D. Sáez-Gómez, Phys. Lett. B **725**, 437 (2013)
3. S. Nojiri, S. Odintsov, V. Oikonomou, Phys. Rep. **692**, 1 (2017)
4. Ö. Akarsu, J.D. Barrow, S. Çıkıntoğlu, K.Y. Ekşi, N. Katırcı, Phys. Rev. D **97**, 124017 (2018)
5. K. Schwarzschild, Sitzungsberichte der königlich preussischen Akademie der Wissenschaften Berlin. Math. Phys. 189 (1916)
6. J.H. Jeans, Mon. Not. R. Astron. Soc. **82**, 122 (1922)
7. R.L. Bowers, E. Liang, Astrophys. J. **188**, 657 (1974)
8. M. Ruderman, Ann. Rev. Astron. Astrophys. **10**, 427 (1972)
9. L. Herrera, N.O. Santos, Phys. Rep. **286**, 53 (1997)
10. W.B. Bonnor, Z. Phys. **160**, 59 (1960)
11. W. Hillebrandt, K.O. Steinmetz, Astron. Astrophys. **53**, 283 (1976)
12. L. Herrera, Phys. Rev. D **101**, 104024 (2020)
13. A. Malik, S. Ahmad, S. Ahmad, New Astron. **79**, 101392 (2020)
14. G. Mustafa, Z. Hassan, P. Moraes, P. Sahoo, Phys. Lett. B **821**, 136612 (2021)
15. M. Bhatti, Z. Yousaf, Chin. J. Phys. **73**, 115 (2021)
16. J. Solanki, Eur. Phys. J. Plus **137**, 557 (2022)
17. Z. Yousaf, M. Bhatti, A. Ali, Ann. Phys. **432**, 168570 (2021)
18. M.Z. Bhatti, M.Y. Khlopov, Z. Yousaf, S. Khan, Mon. Not. R. Astron. Soc. **506**, 4543 (2021)
19. M.Z. Bhatti, Z. Yousaf, S. Khan, Chin. J. Phys. **77**, 2168 (2022)
20. Z. Yousaf, B.M. Z, S. Khan, Ann. Phys. **534**, 2200252 (2022)
21. Z. Yousaf, M.Z. Bhatti, S. Khan, Eur. Phys. J. Plus **137**, 322 (2022)
22. Z. Yousaf, M.Z. Bhatti, S. Khan, Eur. Phys. J. C **82**, 1077 (2022)
23. J.C. Collins, M.J. Perry, Phys. Rev. Lett. **34**, 1353 (1975)
24. N. Itoh, Prog. Theor. Phys. **44**, 291 (1970)
25. R.F. Sawyer, Phys. Rev. Lett. **29**, 382 (1972)
26. J.B. Hartle, R.F. Sawyer, D.J. Scalapino, Astrophys. J. **199**, 471 (1975)
27. L. Celenza, H. Pirner, Nucl. Phys. A **294**, 357 (1978)
28. A. Sokolov, Zhurnal Ehksperimental'noj i Teoreticheskoj Fiziki **49**, 1137 (1980)
29. R. Sawyer, D. Scalapino, Phys. Rev. D **7**, 953 (1973)
30. P. Jones, Astrophys. Space Sci. **33**, 215 (1975)
31. I. Easson, C. Pethick, Phys. Rev. D **16**, 275 (1977)
32. R. Ruffini, S. Bonazzola, Phys. Rev. **187**, 1767 (1969)
33. M. Gleiser, Phys. Rev. D **38**, 2376 (1988)
34. A.N. Kolmogorov, Probab. Inform. Theory J. **1**, 3 (1965)
35. P. Grassberger, Int. J. Theor. Phys. **25**, 907 (1986)
36. S. Lloyd, H. Pagels, Ann. phys. **188**, 186 (1988)
37. X. Calbet, R. López-Ruiz, Phys. Rev. E **63**, 066116 (2001)
38. J. Sañudo, R. López-Ruiz, Phys. Lett. A **372**, 5283 (2008)
39. C.P. Panos, N.S. Nikolaidis, K.C. Chatzisavvas, C. Tsouros, Phys. Lett. A **373**, 2343 (2009)
40. L. Herrera, A. Di Prisco, J. Carot, Phys. Rev. D **99**, 124028 (2019)
41. L. Bel, Ann Inst. H Poincaré **17**, 37 (1961)
42. L. Herrera, J. Ospino, A. Di Prisco, E. Fuenmayor, O. Troconis, Phys. Rev. D **79**, 064025 (2009)
43. Z. Yousaf, Physica Scripta **95**, 075307 (2020)
44. M. Bhatti, Z. Yousaf, F. Hussain, Eur. Phys. J. C **81**, 853 (2021)
45. M.Z. Bhatti, Z. Yousaf, S. Khan, Int. J. Mod. Phys. D **30**, 2150097 (2021)
46. M.Z. Bhatti, Z. Yousaf, S. Khan, Eur. Phys. J. Plus **136**, 975 (2021)
47. Z. Yousaf, M.Z. Bhatti, S. Khan, P.K. Sahoo, Phys. Dark Univ. **36**, 101015 (2022)
48. Z. Yousaf, M.Z. Bhatti, S. Khan, Int. J. Mod. Phys. D **31**, 2250099 (2022)
49. J. Ovalle, in Int. J. Mod. Phys. Conf. Ser., vol. 41 (World Scientific, 2016), p. 1660132
50. J. Ovalle, Phys. Lett. B **788**, 213 (2019)
51. R. Casadio, J. Ovalle, R. Da Rocha, Class. Quantum Gravity **32**, 215020 (2015)
52. J. Ovalle, F. Linares, Phys. Rev. D **88**, 104026 (2013)
53. J. Ovalle, R. Casadio, R. Da Rocha, A. Sotomayor, Eur. Phys. J. C **78**, 122 (2018)
54. L. Gabbanelli, Á. Rincón, C. Rubio, Eur. Phys. J. C **78**, 370 (2018)
55. E. Morales, F. Tello-Ortiz, Eur Phys J. C **78**, 618 (2018)
56. S. Hensh, Z. Stuchlík, Eur. Phys. J. C **79**, 834 (2019)
57. L. Gabbanelli, J. Ovalle, A. Sotomayor, Z. Stuchlik, R. Casadio, Eur. Phys. J. C **79**, 486 (2019)
58. S. Maurya, A. Errehymy, M. Govender, G. Mustafa, N. Al-Harbi, A.-H. Abdel-Aty, Eur. Phys. J. C **83**, 348 (2023)
59. R. Casadio, E. Contreras, J. Ovalle, A. Sotomayor, Z. Stuchlik, Eur. Phys. J. C **79**, 826 (2019)
60. S.K. Maurya, A. Errehymy, R. Nag, M. Daoud, Fortschr. Phys. **70**, 2200041 (2022)
61. S.K. Maurya, M. Govender, S. Kaur, R. Nag, Eur. Phys. J. C **82**, 100 (2022)
62. J. Andrade, Eur. Phys. J. C **82**, 266 (2022)
63. J. Andrade, K.Y. Ortega, W. Klínger, R. Copa, S. Medina, J. Cruz, Eur. Phys. J. C **83**, 1085 (2023)
64. A.M. Albalahi, Z. Yousaf, A. Ali, S. Khan, Eur. Phys. J. C **84**, 9 (2024)
65. L. Herrera, A. Di Prisco, J. Ibanez, Phys. Rev. D **84**, 107501 (2011)
66. J. Ovalle, Phys. Rev. D **95**, 104019 (2017)
67. C.W. Misner, D.H. Sharp, Phys. Rev. **136**, B571 (1964)
68. M.E. Cahill, G.C. McVittie, J. Math. Phys. **11**, 1392 (1970)
69. A. Di Prisco, L. Herrera, G. Le Denmat, M.A.H. MacCallum, N.O. Santos, Phys. Rev. D **76**, 064017 (2007)
70. R.C. Tolman, Phys. Rev. **35**, 875 (1930)
71. S.N. Pandey, S.P. Sharma, Gen. Relativ. Gravit. **14**, 113 (1982)
72. M.K. Jasim, S.K. Maurya, Y.K. Gupta, B. Dayanandan, Astrophys. Space Sci. **361**, 352 (2016)
73. S.K. Maurya, Y.K. Gupta, S. T T, F. Rahaman, Eur. Phys. J. A **52**, 191 (2016)
74. S.K. Maurya, A. Banerjee, M.K. Jasim, J. Kumar, A.K. Prasad, A. Pradhan, Phys. Rev. D **99**, 044029 (2019)